TECHNISCHE UNIVERSITÄT MÜNCHEN

Fakultät für Medizin

Targeting Inflammation in Atherosclerosis Using Colchicine

Clara Ulrike Meyer-Lindemann

Vollständiger Abdruck der von der Fakultät für Medizin der Technischen Universität München zur Erlangung des akademischen Grades einer

Doktorin der Medizinischen Wissenschaften (Dr. med. sci.)

genehmigten Dissertation.

Vorsitz: Prof. Dr. Michael Joner

Prüfer*innen der Dissertation:

1. Prof. Dr. Hendrik Sager

2. Prof. Dr. Lars Mägdefessel

Die Dissertation wurde am 09.02.2023 bei der Technischen Universität München eingereicht und durch die Fakultät für Medizin am 14.06.2023 angenommen.

Table of contents

List of Figures

List of Abbreviations

APC	allophycocyanin
ASC	apoptosis-associated speck-like protein containing a CARD
BMDM	bone marrow derived macrophages
BrdU	bromodesoxyuridin
BW	body weight
CAD	coronary artery disease
CANTOS	Canakinumab Anti-Inflammatory Thrombosis Outcomes Study
CCL-2	CC-Motif Chemokine Ligand 2
CCR1	C-C chemokine receptor type 1
CCR5	C-C chemokine receptor type 5
cDNA	complementary DNA
COLCOT	Colchicine Cardiovascular Outcomes Trial
CVDs	cardiovascular diseases
CX3CL1	C-X3-C motif chemokine ligand 1
CX3CR1	C-X3-C motif chemokine receptor 1
CXCL1	C-X-C motif chemokine 1
CXCL12	CXC motif chemokine ligand 12
CXCL2	C-X-C motif chemokine ligand 2
CXCR2	C-X-C motif chemokine receptor type 2
CXCR4	C-X-C motif chemokine receptor type 4
DNA	desoxyribonucleic acid
ECs	endothelial cells
EDTA	ethylenediaminetetraacetic acid

FACS	fluorescence-activated single cell sorting
FBS	fetal bovine serum
FDA	Food and Drug Administration
GFP	green fluorescent protein
HCD	high cholesterol diet
HEPES)	2-(4-(2-Hydroxyethyl)-1-piperazinyl)-ethansulfonsäure
hsCRP	high-sensitive C-reactive protein
HUVECS	human umbilical vein endothelial cells
ICAM-1	intercellular adhesion molecule 1
ICAM-2	intercellular adhesion molecule 2
Il-18	Interleukin-18
Il-1ß	Interleukin-1ß
Il-6	Interleukin-6
ITGA4	integrin subunit alpha 4
ITGAL	integrin subunit alpha L
ITGAM	integrin subunit alpha M
ITGB1	integrin subunit beta 1
LAD	left anterior descending coronary artery
LDL	low-density lipoprotein
LFA-1	lymphocyte function-associated antigen 1
LoDoCo2	Low-Dose colchicine for Secondary Prevention of Cardiovascular Disease 2
MACE	major adverse cardiac events
M-CSF	macrophage colony-stimulating factor
MFI	mean-fluorescent intensities

MI	myocardial infarction
MMF	mycophenolat-mofetil
MMPs	matrix metalloproteinases
NLRP3	NLR family pyrin domain containing 3
OCT	optimal cutting temperature compound
PAD	peripheral artery disease
PBS	phosphate buffered saline
PECAM1	platelet and endothelial cell adhesion molecule 1
PFA	perfluoroalkoxy alkane
RBC	red blood cell
RNA	ribonucleic acid
RPMI	roswell park memorial institute
TGFβ1	transforming growth factor beta 1
TNF	tumor necrosis factor
VCAM-1)	vascular cell adhesion protein 1
VLA4	integrin alpha 4 beta 1

1 Introduction

1.1 Cardiovascular Disease

Cardiovascular diseases (CVDs) have been the leading cause of death in the Western population for more than 20 years – in 2019 alone, they were responsible for 17.9 million deaths worldwide (WHO, 2019). Shockingly, the prevalence of CVD has nearly doubled in the past 30 years and currently stands at 523 million cases worldwide (Roth *et al.*, 2020). Coronary artery disease (CAD), peripheral arterial disease (PAD), stroke, and myocardial infarction (MI), among others, belong to the disease spectrum. Common feature is the underlying pathophysiological mechanism: atherosclerosis.

1.2 Atherosclerosis

1.2.1 Pathogenesis

Atherosclerosis is a chronic inflammatory disease of the vessel wall leading to the formation of lipid-containing plaques in the intima, the innermost layer of the vessel wall (Libby *et al.*, 2019a). Pathogenetically, atherosclerosis is the result of metabolic and inflammatory pathways, that are indispensably entangled (Wolf and Ley, 2019). As shown in **Figure 1,** high plasma lipid levels as well as hemodynamic shear stress provoke the functional impairment of the endothelium, the interior surface of the intima established by a single layer of endothelial cells (ECs) (Galley and Webster, 2004). The functional impairment of the endothelium provokes an increased vascular permeability allowing the subendothelial deposition of low-density lipoproteins (LDL) (Libby *et al.*, 2019a). Further, it promotes the recruitment of inflammatory leukocytes into atherosclerotic plaques by enhancing endothelial expression of leukocyte adhesion molecules as well as increasing the release of leukocyte-attracting cytokines (Mauersberger *et al.*, 2021). The intraplaque accumulation of monocytes, neutrophils and T-cells provokes a pro-inflammatory, disease-propagating environment (Ley and Reutershan, 2006, Soehnlein and Libby, 2021). Intramurally, monocytes differentiate into mature macrophages, the major leukocyte population in plaque (Zernecke *et al.*, 2020). The intracellular uptake of oxidized LDL

encourages the development of macrophages into lipid-laden foam cells (Yu *et al.*, 2013). The accumulation of foam cells provokes the formation of fatty streaks, representing the macroscopically visible correlate of atherosclerosis. Further uptake of LDL induces the establishment of an inner necrotic core where dying cells accumulate and release intracellularly enriched lipids, thus further promoting inflammatory reactions. The atherosclerotic plaque is surrounded by a thin fibrous cap made up of intimal smooth muscle cells and connective tissues (Falk, 2006, Libby *et al.*, 2019a). The fibrous cap critically influences plaque stability and, consequently, the risk for plaque rupture (Li *et al.*, 2006) or erosion (Libby *et al.*, 2019b).

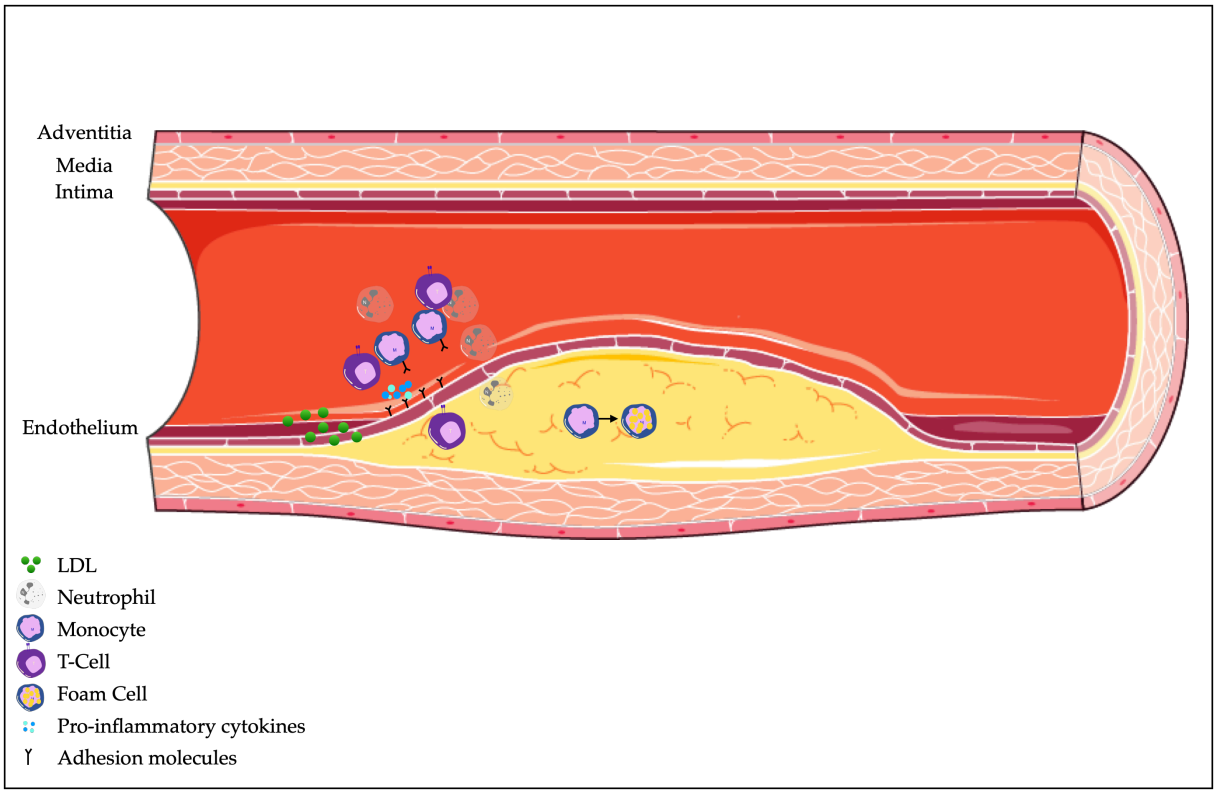

Figure 1: Pathogenesis of atherosclerosis

Initially, due to functional impairment of the endothelium, circulating low-density lipoproteins (LDL) infiltrate the vessel wall, particularly in regions with disturbed flow. Further, the recruitment of leukocytes into the atherosclerotic plaque is enhanced because of an increased expression of leukocyte adhesion molecules as well as an enhanced release of leukocyte-attracting cytokines. Once migrated into the plaque, monocytes differentiate into macrophages and strongly ingest LDL, thereby developing into foam cells, macroscopically visible as fatty streaks.

1.2.2 Symptoms

Usually, symptoms occur late and allow undetected progression over years. However, if the formed plaques exceed a certain degree of stenosis, they may become clinically

apparent because of ischemia-related pain. Due to intraluminal obstruction, the circulating blood flow is not sufficient to fully maintain tissue perfusion. Thus, atherosclerosis can cause organ-related partial functional impairment (= stenosis) or even complete functional loss (= occlusion). The main sites of plaque formation are the abdominal aorta, coronary arteries, popliteal arteries, internal carotid arteries, as well as the circulus arteriosus cerebri. Consequently, particularly vital organs such as the heart, brain, and kidneys are jeopardized by atherosclerosis. Depending on the localization, different clinical pictures are caused. Plaque formation within the coronaries is the basis of CAD. The increased oxygen demand of the myocardium during physical and/ or mental stress cannot be met due to narrowing of the supplying vessels. Lack of oxygen provokes stress-dependent thoracic pain, so-called angina pectoris. Further, atherosclerosis can become clinically apparent by plaque rupture or erosion, which triggers atherothrombosis and may result in occlusion of the affected or more distal vessels, causing life-threatening emergencies such as MI or stroke (Libby *et al.*, 2019a, Libby *et al.*, 2019b).

1.2.3 Therapy

To avoid these fatal consequences, early and effective therapy of atherosclerosis is crucial. As mentioned above, hemodynamic, and biochemical-toxic stress operate as first catalysts of atherosclerosis. Hence, addressing these modifiable risk factors is the rationale for preventive and therapeutic measures. Healthy, balanced nutrition, regular exercise as well as nicotine avoidance protect against dyslipidemia, arterial hypertension, diabetes mellitus as well as obesity (Visseren *et al.*, 2022). However, lifestyle changes are challenging to implement as they are often a major constraint from the patient's perspective – while at the same time their effectiveness is strongly correlated with patient compliance (Burgess *et al.*, 2017). If the effect of lifestyle intervention is insufficient or if the risk profile is correspondingly high, additional drug therapy should be established. Since LDL is the most important modifiable risk factor, the use of cholesterol-lowering drugs like statins plays a particularly important role (Libby *et al.*, 2019a, Visseren *et al.*, 2022). Further, pharmacological therapy should be initiated to treat arterial hypertension and diabetes mellitus.

1.2.4 Challenges

Despite these established therapy concepts, CVD remain the leading causes of death in the world entailing rising health care costs (Roth *et al.*, 2020). Affected patients suffer from reduced quality of life and experience long periods of hospitalization and limited participation in society. Although therapeutic interventions for secondary prevention may decelerate atherosclerosis, disease progression continues inexorably even with well-controlled lipid levels (Libby and Everett, 2019). Numerous preventable deaths highlight the urgent need of establishing innovative therapeutic options.

1.3 Inflammation in atherosclerosis

Recently, several studies demonstrated that inflammation plays an important role in the pathogenesis of atherosclerosis (Libby *et al.*, 2009).

1.3.1 Inflammatory cells

Circulating blood leukocytes, the executive forces of the immune system, act as a risk factor and prognostic indicator for atherosclerosis (Madjid *et al.*, 2004, Swirski and Nahrendorf, 2013). Because monocytes and neutrophils are short-lived (<72 hours), their abundance in the circulation as well as their recruitment to cardiovascular organs is highly dependent on their production rate (Nahrendorf and Swirski, 2015). Regularly, hematopoiesis is situated in the bone marrow. Inflammatory diseases like atherosclerosis additionally stimulate extramedullary hematopoiesis, primarily located in the spleen (Robbins *et al.*, 2012, Dutta *et al.*, 2015). After their release into the bloodstream, leukocytes are recruited to the plaque and contribute to all stages of disease by fostering a pro-inflammatory milieu (Mauersberger *et al.*, 2021). The intraplaque expansion of leukocytes is further achieved by *in-situ* proliferation. The leukocyte supply chain is pictured in **Figure 2**.

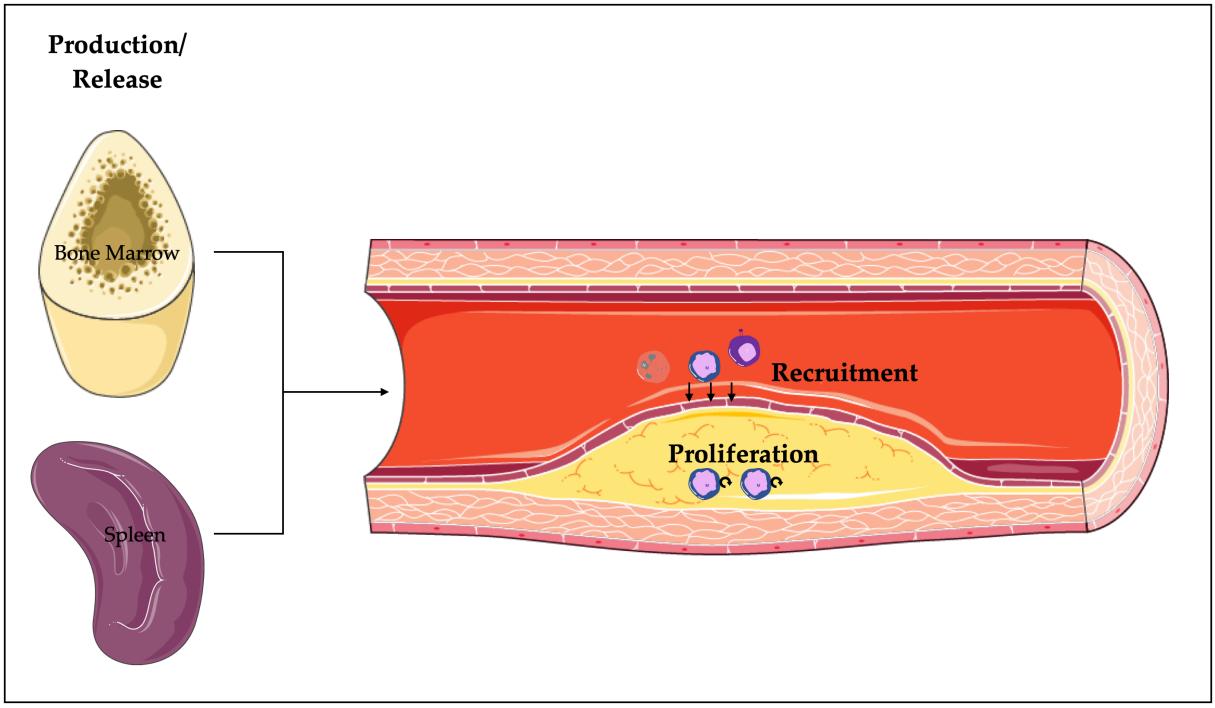

Figure 2: The leukocyte supply chain

Leukocytes are produced in the bone marrow and spleen, released into the blood, recruited to the plaque, and can expand locally by *in-situ* proliferation.

1.3.2 Cytokines

To orchestrate the complex interactions between leukocytes, cell-derived mediators called cytokines serve as messenger substances. Interleukins and interferons act as signaling molecules for the intercellular communication and are fundamental to regulate proliferation, differentiation, and function of leukocytes (Kleemann *et al.*, 2008). Chemokines, on the other hand, are mediators for the attraction of leukocytes to inflammatory tissues. Besides, they are implicated in the uptake of leukocytes from the blood to peripheral tissues (Ramji and Davies, 2015).

1.3.3 The inflammasome

Inflammasomes are cytosolic multiprotein complexes composed of the sensor protein NLR family pyrin domain containing 3 (NLRP3), the adaptor protein apoptosis-associated speck-like protein containing a CARD (ASC), and procaspase-1 (Guo *et al.*, 2015). Inflammasomes are predominantly expressed in macrophages to initiate inflammatory responses through cytokine release (Rathinam and Fitzgerald, 2016, Karasawa and

Takahashi, 2017). As shown in **Figure 3**, atherosclerosis-associated stimuli such as hypoxia, cholesterol crystals, or disturbed flow (co-)activate NLRP3 provoking the release of caspase-1, the enzyme catalyzing the maturation of interleukin-1ß (Il-1ß) and interleukin-18 (Il-18) (Libby and Everett, 2019). Il-1ß accelerates atherosclerosis progression by inducing the production of interleukin-6 (Il-6) in the liver. The provoked acute phase response allows the release of more than 30 pro-inflammatory and procoagulant proteins. Ultimately, the activation of the NLRP3 inflammasome results in enhanced atherothrombosis (Abbate *et al.*, 2020).

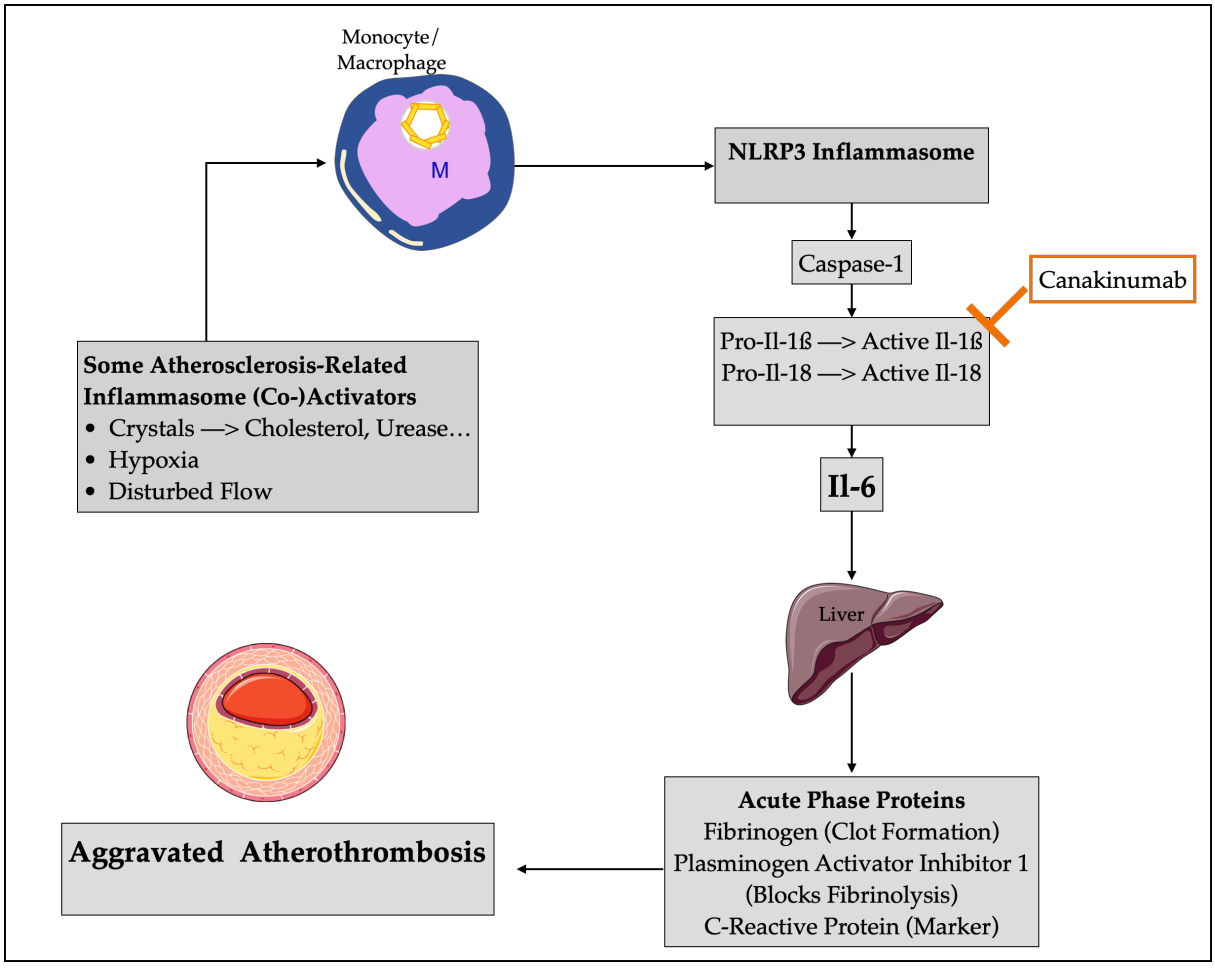

Figure 3: The NLRP3 Inflammasome

The NLR family pyrin domain containing 3 (NLRP3) inflammasome can be activated by atherosclerosis-related stimuli like cholesterol crystals or disturbed flow. Activation promotes the release of caspase-1, the enzyme catalyzing the maturation of interleukin-1ß (Il-1ß) and interleukin-18 (Il-18). Il-1ß stimulates the production of Interleukin-6 (IL-6) in the liver initiating an acute phase response stimulating the release of more than 30 pro-inflammatory and procoagulant proteins. Ultimately, activation of NLRP3 inflammasome promotes aggravated atherothrombosis. Modified from (Libby and Everett, 2019).

1.4 Targeting inflammation in atherosclerosis

As inflammation strongly contributes to atherosclerotic disease progression, targeting inflammatory pathways represents a promising preventive and therapeutic approach to combat atherosclerosis. The clinical proof of principle was first achieved in 2017 by the Canakinumab Anti-Inflammatory Thrombosis Outcomes Study (CANTOS). This randomized, double-blinded trial enrolled more than 10.000 patients who met the criteria of recent MI (>30 days) plus systemic inflammation determined as elevated high-sensitive C-reactive protein (hsCRP) >2 mg/l. Subcutaneous treatment for 3 months with canakinumab, an Il-1ß inhibitor, significantly reduced the incidence of major cardiovascular events in these patients compared with placebo. In fact, those patients with the greatest reduction of systemic inflammation (= greatest reduction of hsCRP) benefited the most (Ridker *et al.*, 2018). Because Canakinumab acts independently of lipid metabolism and blood pressure, the CANTOS trial promoted inflammation as a new druggable target in the treatment of atherosclerosis (Ridker *et al.*, 2017). Despite this great scientific gain, there are some non-negligible challenges: Canakinumab must be applied subcutaneously, costs about $200,000 a year, and carries serious side effects including risk of fatal infections (Nidorf and Thompson, 2019). Furthermore, canakinumab has not been approved by the Food and Drug Administration (FDA) for the treatment of atherosclerosis (Bell, 2018). This urgently requires the search for cheap, safe, and simple alternatives to successfully target inflammation in atherosclerosis.

1.4.1 Colchicine

Colchicine, a derivative of *Colchicum autumnale*, is an orally administered drug, whose anti-inflammatory mode of action is used in the treatment of gout, familial Mediterranean fever, and pericarditis (Deftereos *et al.*, 2013). With costs of approximately $0.26 per pill, it is an inexpensive, widely available drug (Samuel *et al.*, 2021).

1.4.1.1 Mechanism of action

Colchicine acts – unlike many other anti-inflammatory drugs – independent of the arachidonic metabolism as it inhibits microtubule assembly (Deftereos *et al.*, 2013). Being an essential component of the cytoskeleton, microtubules are responsible for the stability

of cells, but also play an essential role in dynamic cellular processes (Goodson and Jonasson, 2018). Incorporation of colchicine in the alpha-beta subunit of tubulin, the major component of microtubules, induces a dosage-dependent depolymerization of microtubules suppressing cell mitosis, exocytosis, and neutrophil motility (Deftereos *et al.*, 2013). Thereby, colchicine indirectly hinders activation of the NLRP3 inflammasome as microtubules are responsible for the assembly-required transport of NLRP3 and its adaptor into the endoplasmic reticulum (Pascart and Richette, 2018). Furthermore, colchicine inhibits the upstream production of Il-1ß (Martinon *et al.*, 2006). These mechanisms of action have largely been identified in the context of gout because, as mentioned above, colchicine is used here as a standard therapeutic agent (Pascart and Richette, 2018). Even though they are phenotypically entirely different diseases, gout and atherosclerosis are based on similar pathogenesis, such as cholesterol crystal-induced activation of the NLRP3 inflammasome (Nidorf and Thompson, 2019, Strandberg and Kovanen, 2021), raising the question of whether colchicine could also be used to target inflammation in the setting of CVD.

1.4.1.2 Colchicine in the context of CAD

Indeed, clinical trials have already demonstrated the efficacy of colchicine in cardiovascular disease. In the Colchicine Cardiovascular Outcomes Trial (COLCOT) published in 2019, 4745 patients were treated with 0.5mg colchicine or placebo once daily shortly after MI (<30 days) in addition to guideline-directed drug therapy. The colchicine group showed a significantly lower risk of ischemic cardiovascular events (5.5% versus 7.1%) particularly through a reduction in strokes (Tardif *et al.*, 2019). These promising results were further confirmed by the Low-Dose Colchicine for Secondary Prevention of Cardiovascular Disease 2 Trial (LoDoCo2) published in 2020. Here, 5522 patients with chronic stable CAD were treated once daily with 0.5 mg colchicine or placebo. After an average follow-up of 28.6 months, the colchicine group showed a reduced risk of cardiovascular events of 6.8% in comparison to 9.6% in the vehicle group (Nidorf *et al.*, 2020b). Both trials reveal the great potential of colchicine in secondary prevention therapy for atherosclerosis. Furthermore, a meta-analysis from 2021 reported that colchicine reduced the incidence of major adverse cardiac events (MACE) (the composite of MI,

stroke, and cardiovascular death) by 25%. Thus, colchicine achieves similar effects to lipid-lowering and anti-thrombotic therapies in terms of cardiovascular risk reduction (Fiolet *et al.*, 2021). However, it remains unclear, how exactly colchicine exerts its anti-inflammatory properties in the context of CAD.

1.5 Aim

Targeting vascular inflammation in atherosclerosis provides a novel therapeutic approach to beneficially alter the course of disease. Colchicine, a microtubule inhibitor with anti-inflammatory properties, represents a potentially useful agent as it led to a reduction of cardiovascular events in patients with recent acute coronary syndrome and chronic coronary disease (Tardif *et al.*, 2019, Nidorf *et al.*, 2020b). However, the mechanistic basis of these observations remains elusive. The hypothesis of this doctoral thesis is that colchicine prevents the expansion of pro-inflammatory leukocytes within the plaque leading to reduced vulnerability in plaque. First, it will be investigated whether anti-inflammatory colchicine influences the leukocyte supply chain in mice. Subsequently, underlying mechanisms will be identified.

2 Methods

2.1 Mouse Studies

To study atherosclerosis in mice, the *Apoe*$^{-/-}$ (B6.129P2-Apoetm1Unc/J) mouse model (Lo Sasso *et al.*, 2016) was used. C57Bl/6 J mice were used for cell culture experiments. Additionally, the expression of green fluorescent protein of *Ubc-GFP* mice (C57BL/6-Tg(UBC-GFP)30Scha/J) was exploited for *in vivo* leukocyte tracking experiments. *Apoe*$^{-/-}$ and *Ubc-GFP* mice were purchased from The Jackson Laboratory (Bar Harbor, ME, USA) and expanded by in-house breeding. C57BL/6 J mice were ordered from Charles River Laboratories (Sulzfeld, Germany). Age- and sex-matched littermates were used for all experiments and assignment to groups was random. All experiments were conducted in accordance with the German legislation on protection of animals and approved by the local animal care committee (AZ: ROB-55.2-2532.Vet_02-16-92).

2.1.1 Experimental set-up: atherosclerosis

For initiation and progression of atherosclerotic plaques, 8-week-old *Apoe*$^{-/-}$ mice were fed a high cholesterol diet (HCD, 21.2% fat by weight and 0.2% cholesterol, TD.88137, Envigo, Indianapolis, IN, USA) over a period of 8 weeks.

2.1.1.1 Treatment with vehicle/colchicine

During the last four weeks of HCD, a sterile solution of vehicle (phosphate buffered saline (PBS) or colchicine (dissolved in sterile PBS, 0.25 mg/kg bodyweight (BW), C3915, Sigma-Aldrich, St. Louis, MO, USA) was injected intraperitoneally once daily. The dosage of colchicine was adjusted to recently published experiments (Akodad *et al.*, 2017), (Fujisue *et al.*, 2017). Colchicine was kept protected from light. The experimental scheme is portrayed in **Figure 4**.

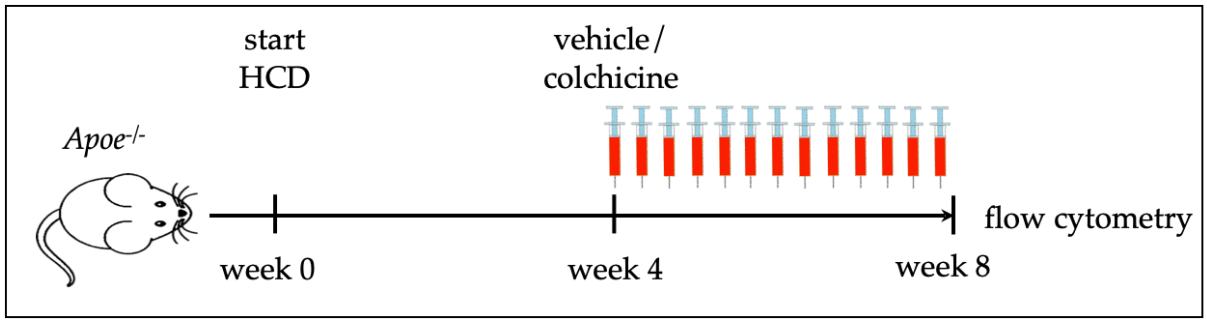

Figure 4: Experimental scheme: atherosclerosis

8-week-old *Apoe*$^{-/-}$mice were subjected to a cholesterol-enriched diet (high cholesterol diet, HCD) for a period of 8 weeks and treated daily with intraperitoneal injections of either vehicle or colchicine (0.25 mg/kg BW) in the last 4 weeks of HCD. Reprinted under the terms of the Creative Commons CC BY license: Supplementary Figure 1A from reference (Meyer-Lindemann *et al., 2022).*

2.1.2 Experimental set-up: MI-accelerated atherosclerosis

To investigate the effect of colchicine on MI-accelerated atherosclerosis, *Apoe*$^{-/-}$ mice underwent surgical induced MI after 4 weeks of feeding with HCD. MI was caused via permanent occlusion of the left anterior descending coronary artery (LAD), supplying the anterior wall of the left ventricle.

2.1.2.1 MI surgery

Specifically, mice were operated under a midazolam (5.0 mg/kg BW), medetomidine (0.5 mg/kg BW), and fentanyl (0.05 mg/kg BW) anesthesia. After thoracotomy in the left intercostal space, the LAD was displayed under microscopic view. An 8-0 prolene was used to permanently suture the LAD, thereby restricting blood flow and oxygen supply to the left ventricle, causing myocardial infarction. The operation was performed by Xinghai Li (German Heart Centre Munich). For subsequent analgesic therapy, mice were treated with subcutaneous injections of buprenorphine every 8 hours for a period of 3 days. After one week of recovery, mice received daily injections of PBS or colchicine as described above. The HCD was maintained throughout the experiment. The experimental scheme is displayed in **Figure 5.**

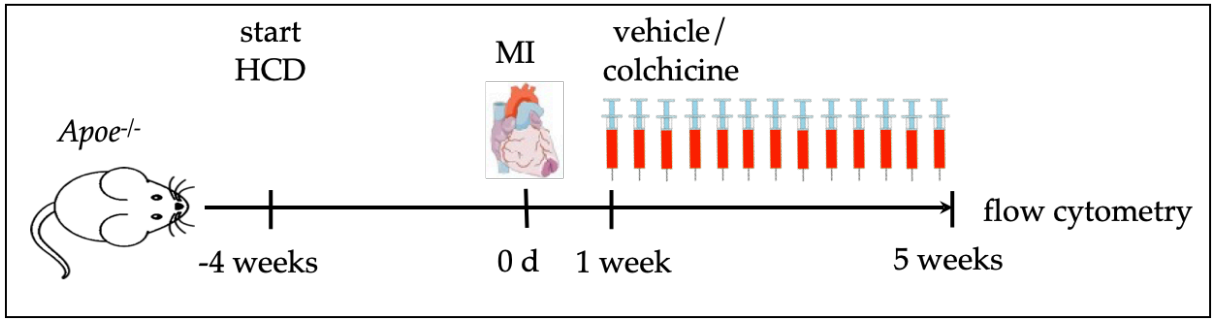

Figure 5: Experimental scheme: MI-accelerated atherosclerosis

Apoe$^{-/-}$ mice on a high cholesterol diet (HCD) were subjected to myocardial infarction (MI) and treated with either vehicle or colchicine for four weeks starting one week after induction of MI.

2.1.3 Tissue collecting

On the day of harvest, mice were initially sedated in an isoflurane chamber. For *in vivo* staining of circulating blood leukocytes, an antibody targeting CD45-BV605 (clone 30-F11, 1:10 in 100 µl PBS, BioLegend, San Diego, CA, USA) was injected intravenously 5 min before euthanizing the animals. After determination of the body weight (BW), a blood sample was drawn retrobulbar. The collected blood was transferred to ethylenediaminetetraacetic acid (EDTA) coated tubes for plasma collection and to fluorescence-activated single cell sorting (FACS) tubes for flow cytometric analysis, respectively. Mice were then placed in the supine position and a skin incision was made at the sternal level followed by opening of the thoracic cavity. After transection of the inferior vena cava, retrograde irrigation of the aorta was performed by puncturing the right ventricle with a 20 ml syringe. Following the extension of the skin incision abdominally, the organs of the gastrointestinal tract were removed, and the spleen was carefully dissected free. Subsequently, the spleen was weighted and then processed through a 40 µm cell strainer to obtain a single cell suspension. By microscope assistance, the aorta was carefully cleaned from fat and tissue and then extracted from root to common iliac artery bifurcation. Bone marrow was sampled from femurs by flushing the bones with PBS after opening the medullary level. The obtained cells were filtered using a 40 µm cell strainer.

2.1.4 Tissue processing

Lysis of erythrocytes was performed in both blood and spleen samples by applying 1X red blood cell (RBC) lysis buffer for 5 min (420302, BioLegend). After stopping the reaction with PBS, the samples (blood, spleen, and bone marrow) were centrifuged at 400xg for 8 min at 4 °C and resuspended in FACS Buffer (PBS containing 0.5% bovine serum albumin, A2153, Sigma). Cells were then filtered using a 40 μm cell strainer. Aortas were minced in respective digestion buffer composed of collagenase I (450 U/ml, C0130), collagenase XI (125 U/ml, C7657), DNase I (60 U/ml, D5319-500UG), and hyaluronidase (60 U/ml, H3506, all Sigma Aldrich) and PBS. Samples were incubated for 1 h under agitation at 37 °C. For analysis of aortic ECs, digestion buffer consisted of PBS containing DNase I (250 U/ml) and collagenase IV (2500 U/ml, LS004212, CellSystems) and the digest was carried out for 40 min at 37 °C. Subsequently, cell suspensions were filtered using a 40 μm cell strainer and resuspended in FACS buffer.

2.1.5 Flow cytometry

After creating single cell suspensions as described above, all samples were stained using fluorescently labeled antibodies as stated below for 15 min at 4 °C in 300 μl FACS buffer. Then, cell suspensions were washed by adding 1 ml of FACS buffer and centrifugation at 400xg for 8 min at 4 °C. Samples were subsequently submitted to flow cytometric analysis on a BD LSRFortessa (BD Biosciences) and files were analyzed using FlowJo software (version 9).

2.1.5.1 Myeloid Cells

To analyze the myeloid cell subset, cells were stained with anti-mouse hematopoietic lineage markers and leukocyte subset markers as listed in **Table 1**. Based on size and granularity, forward versus sideward scatter (FSC vs. SSC) gating was used to sort cells of interest, while duplicates were removed. Myeloid cells were further characterized as follows: neutrophils as lineage^{high}CD45.2^{high}CD11b^{high}CD115^{low}Ly6C^{intermediate}, monocytes as lineage^{low}CD45.2^{high}CD11b^{high}F4/80^{low}Ly6C$^{high/low}$ (in aortic cell suspensions) or lineage^{low}CD45.2^{high}CD11b^{high}CD115^{high}Ly6C$^{high/low}$ (in blood), and macrophages as lineage^{low}CD45.2^{high}CD11b^{high}Ly6C$^{low/intermediate}$F4/80^{high}. *In vivo* labeling, i.e., by

intravenously injecting CD45 5 min before the harvest, allowed to distinguish blood cells ($CD45^+$) from aortic cells ($CD45^-$) and to exclude a possible blood contamination

Table 1: Flow cytometry antibodies used for mouse myeloid cell analysis

Target	Conjugate	Manufacturer	Catalogue#	Clone	Dilution
B220	PE	Biolegend	103208	RA3-6B2	1:600
CD90.2	PE	Biolegend	140308	53-2.1	1:300
CD49b	PE	Biolegend	140308	DX5	1:1200
NK1.1	PE	Biolegend	108708	PK136	1:600
Ter-119	PE	Biolegend	116208	TER-119	1:600
Ly6G	PE	Biolegend	127608	1A8	1:600
CD45.2	PerCP/Cy5.5	Biolegend	109828	104	1:300
CD11b	APC/Cy7	Biolegend	101226	M1/70	1:600
CD115	BV711	Biolegend	135515	AFS98	1:600
F4/80	PE/Cy7	Biolegend	123114	BM8	1:600
Ly6C	FITC	Biolegend	128006	HK1.4	1:600
	BV421	Biolegend	128032		

2.1.5.2 Endothelial Cells

For aortic EC analysis and sorting, staining was performed using the antibodies listed in **Table 2**. ECs were characterized as $CD45.2^{low}$, $CD31^{high}$, and $CD107^{middle/high}$. Expression of adhesion molecules was quantified by appropriate histograms.

Table 2: Flow cytometry antibodies used for aortic EC analysis and sorting

Target	Conjugate	Manufacturer	Catalogue#	Clone	Dilution
CD54 (ICAM1)	APC	Biolegend	116120	YN1/1.7. 4	1:600
CD102 (ICAM2)	Biotin	Biolegend	105604	3C4	1:600
CD106 (VCAM1)	PE/Cy7	Biolegend	105720	429	1:300
CD62E (E-selectin)	PE	Biolegend	55375	RB40.34	1:300
CD62P (P-selectin)	FITC	Biolegend	553744	RB40.34	1:300
CD31	BV421	Biolegend	102424	390	1:600
CD107a (LAMP-1)	APC/Cy7	Biolegend	121616	1D4B	1:300
CD45. 2	PerCP/Cy5.5	Biolegend	109828	104	1:300
Streptavidin	BV510	Biolegend	405234		1:300

2.1.5.3 Fluorescence-activated cell sorting

Blood leukocytes and aortic ECs were sorted on a FACS Aria III using FACSDiva Software version 6 (BD Biosciences) by Dr. Michael Hristov (LMU Munich). Neutrophils were characterized as $CD45.2^{high}CD11b^{high}lineage^{high}CD115^{low}Ly6C^{intermediate}$, $Ly6C^{high}$ and $Ly6C^{low}$ monocytes as $CD45.2^{high}CD11b^{high}lineage^{low}CD115^{high}Ly6C^{high/low}$, and ECs as $CD45.2^{low}CD31^{high}$ cells. Cells were directly sorted into RNA extraction buffer (KIT0204, Thermo Fisher Scientific) containing tubes and snap-frozen to -80°C.

2.1.5.4 Flow cytometric visualization of proliferating cells

To investigate the proliferation of bone marrow derived macrophages (BMDM), a bromodesoxyuridin (BrdU) staining was used. The exact experimental setup of the *in vitro* experiment is explained in the section Cell culture. BrdU, a chemical analog of thymidine or deoxyuridine, can be incorporated into the DNA of proliferating cells which can be visualized by flow cytometry. Cells were first stained with antibodies targeting the cell-surface markers CD45.2, CD115, Ly6C and F4/80 for 15 min at 4 °C in 300 µl FACS buffer. The antibodies used are listed in **Table 1.** To enable the incorporation of BrdU, cells were fixed using 100 µl of BD Cytofix/Cytoperm (554714 BD Biosciences) for 30 min at 4 ° C. Then, cell suspensions were washed by adding 1x BD Perm/Wash Buffer (554723, BD Biosciences) and centrifugation at 400xg for 8 min at 4 °C. Cells were resuspended in 100 µl of a 1mg/ml solution of DNAse (D4513, Sigma Aldrich) and incubated for 1 h at 37 °C. Subsequently, cells were washed by adding 1x BD Perm/Wash Buffer (554723, BD Biosciences) and centrifugation at 400xg for 8 min at 4 °C. Cells were stained in 50 µl of BD Perm/Wash Buffer containing 1 µl of Allophycocyanin (APC)-conjugated anti-BrdU antibody (552598, BD Biosciences) and submitted to flow cytometric analysis.

2.1.6 Adoptive transfer of green fluorescent protein (GFP)-labeled neutrophils and monocytes

To analyze the recruitment of leukocytes, an adoptive transfer was performed. Hereby, green-fluorescent bone marrow cells from *Ubc-GFP* donor animals were obtained and converted into single cell suspensions as described in the section Tissue processing. Since only neutrophils and monocytes were to be transferred from the donor to the recipient animals, purification of the cell suspension had to be carried out first. Neutrophils and monocytes were stained with Ly6G-PE (Clone 1A8) and CD115-biotin (clone AFS98, both BioLegend) for 15 min and excess antibody was removed by adding 1 ml of FACS buffer and centrifuging samples for 8 min at 400xg. The antibodies were then coupled to magnetic beads (anti-PE and streptavidin microbeads, Miltenyi Biotec, Bergisch Gladbach, Germany) for another 15 min as stated above. Subsequently, the cell suspension was placed on magnetic-activated specific columns (130-042-401, Miltenyi Biotec). The magnetically labeled cells were retained in the column by the magnetic field, and the non-

magnetically labeled cells were discarded as flow-through. The column was then removed from the magnetic holder and the cells were flushed into a new tube with PBS. Equal amounts of the isolated cells were injected intravenously into *ApoE*$^{-/-}$ mice 24 h before harvest. Quantification of recruited CD11b^{high}GFP^{high} cells within aortas as well as the degree of purification of the separated cells were detected by flow cytometry. The experimental scheme is displayed in **Figure 6**.

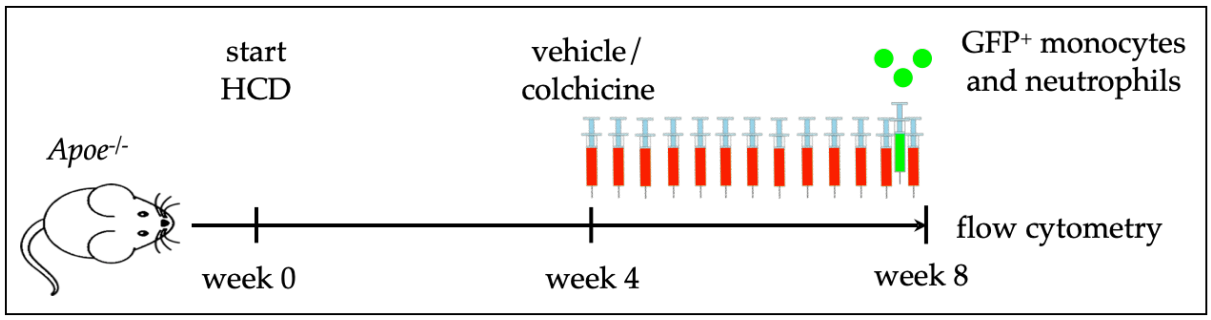

Figure 6: Experimental scheme: adoptive transfer of green fluorescent protein (GFP)-labeled neutrophils and monocytes

After treatment with vehicle/ colchicine for 4 weeks, GFP^{high} monocytes and neutrophils were intravenously injected into *Apoe*$^{-/-}$ mice 24 hours before the harvest. Reprinted under the terms of the Creative Commons CC BY license: Supplementary Figure 1C from reference (Meyer-Lindemann *et al., 2022*).

In addition, the recruitment behavior of vehicle or colchicine-treated GFP^{high} leukocytes, respectively, was examined as shown in **Figure 7**. Here, leukocytes were isolated from *Ubc-GFP* mice previously treated with vehicle or colchicine for one week and then adoptively transferred into *Apoe*$^{-/-}$ mice. 24 h later, GFP^{high} leukocytes were quantified in aortic suspensions by flow cytometry which were obtained as stated in the sections Tissue collecting and Tissue processing.

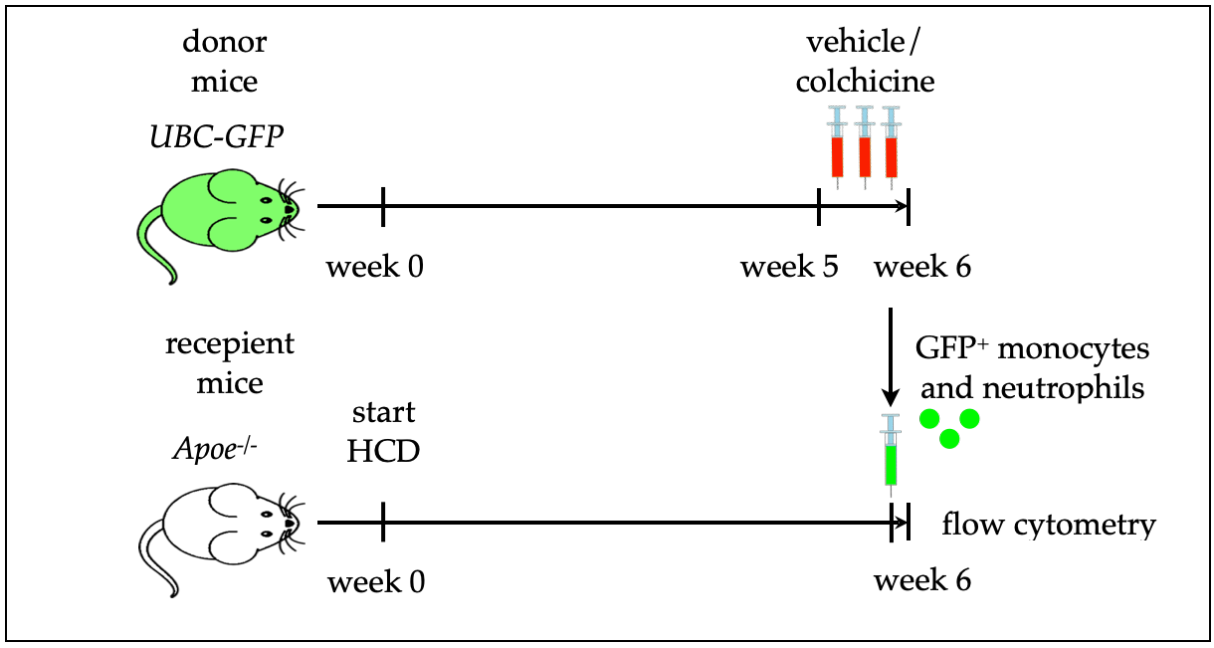

Figure 7: Experimental scheme: adoptive transfer of green fluorescent protein (GFP)-labelled neutrophils and monocytes exposed to vehicle/colchicine

GFP^{high} monocytes and neutrophils isolated from vehicle- or colchicine-treated *UBC-GFP* mice, respectively, were intravenously injected into *Apoe*$^{-/-}$ mice that received a cholesterol-enriched diet (high cholesterol diet, HCD for 8 weeks 24 h before the harvest. Reprinted under the terms of the Creative Commons CC BY license: Figure 3A from reference (Meyer-Lindemann *et al., 2022).*

2.1.7 Histology

For histologic evaluation, aortic roots were excised posterior to the aortic valve by help of a microscope. They were then embedded in dishes with optimal cutting temperature compound (OCT) (Sakura Finetek, Tokyo, Japan) and stored at -80 °C. Subsequently, samples were cut into 5 µm cross-sections using a cryostat (Leica CM3050S). Per mouse and per staining, 3 to 5 sections were examined at 25 µm intervals.

2.1.7.1 Masson-Trichrome

The absolute size of the plaques was estimated by Masson trichrome staining (HT15-1KT, Sigma Aldrich). 5 µm cross-sections were fixed in a 4% solution of paraformaldehyde (PFA) for 45 s and then immersed in distilled water for 60 s. Slides were pickled in preheated Bouin's solution (HT10132, Sigma Aldrich) at 56 ° C for 15 min and then cooled in warm tap water. The sections were washed in running tap water for 2-3 min and then

stained. First, they were stained in Weigert's Hematoxylin Solution (HT1079, Sigma Aldrich) for 5 min, then washed in warm running tap water for 5 min and then rinsed in distilled water. Subsequently, sections were stained in Biebrich-Scarlet-Acid Fuchsin (HT151, Sigma Aldrich) for 5 min and then rinsed well in distilled water. The slides were placed in Phosphotungstic/Phosphomolybdic Acid Solution (HT153, Sigma Aldrich) and Aniline Blue Solution (B8563, Sigma Aldrich), respectively, for 5 min. Then, slides were placed in Acetic Acid 1% for 2 min. For dehydration, slides were first rinsed in distilled water, and then placed in Ethanol 70%, followed by Ethanol 96%, and finally Ethanol 100%. Slides were then cleared and washed in Xylol. A drop of mounting medium (41-4011-00, Medite Cancer Diagnostics) was placed on the slide, which was then covered with a glass slip. Quantification of plaque area (in μm^2) for sections showing two complete cusps was analyzed using ImageJ. Based on the evaluated images, an average value was calculated for each mouse.

2.1.7.2 Immunohistology

To analyze the distribution of $CD11b^+$ cells and $Ly6G^+$ cells, 5 µm cross sections were first fixed in ice-cold acetone for 10 min (6474.1, Roth). Sections were then stained with an anti-CD11b antibody (101202, BioLegend, dilution 1:200)/anti-Ly6G antibody (clone 1A8, BioLegend, dilution 1:200) followed by a staining with a biotinylated secondary antibody (BA-4001, Vector Laboratories, dilution 1:200). To visualize the coupled antibodies, the VECTASTAIN ABC kit (PK-4000, Vector Laboratories) was used in combination with AEC substrate (K3461, Dako). Cell nuclei were counterstained with Gill's hematoxylin solution no. 2 for 2 min (1051752500, Merck Millipore). Slides were mounted using Kaiser's glycerol gelatin. Sections were analyzed by quantifying the CD11b and Ly6G positive area per total plaque area using ImageJ software.

2.1.8 Isolation of nucleic acids and real-time quantitative polymerase chain reaction (qPCR)

After careful removal, aortic arches and spleens were dissociated in 500 µl Qiazol lysis reagent (Qiagen; Hilden, Germany) using a mechanical disruptor (TH220) equipped with soft tissue tips (all OMNI International, Kennesaw, GA, USA). Total ribonucleic acid

(RNA) was extracted by using the RNeasy Mini Kit (Qiagen) in accordance with the manufacturer´s instructions, extended by an additional desoxyribonucleic acid (DNA) removal step (RNase-free DNase set, Qiagen). RNA of FACS-sorted leukocytes and aortic ECs was isolated according to the manufacturer's instructions (PicoPure™ RNA Isolation Kit, Thermo Fisher Scientific). The quality of the extracted RNA was determined using a NanoQuant Plate on an Infinite M200 PRO plate reader (both TECAN, Männedorf, Switzerland). Synthesis of complementary DNA (cDNA) was carried out by using the High-Capacity RNA-to-cDNA kit (Applied Biosystems, Waltham, MA). The cDNA reaction mix was prepared according to **Table 3.**

Table 3: Preparation of cDNA synthesis reaction

Volume (per sample)	**Reagent**
10 µl	2X RT Buffer Mix
1 µl	20X RT Enzyme Mix
25 ng	RNA sample
ad 20 µl	UltraPure Distilled Water

Real-time qPCR was performed using the TaqMan probes displayed in **Table 4** and the TaqMan Fast Universal PCR Master Mix (4352042; all Thermo Fisher Scientific, Waltham, MA, USA). Over 40 cycles on a ViiA 7 system were carried out separately for each gene of interest. The cycling conditions are displayed in **Table 5**. Glyceraldehyde 3-phosphate dehydrogenase (*Gapdh)* served as a housekeeping gene and data were converted to $2^{-\Delta\Delta Ct}$ values.

Table 4: TaqMan Probes used for qPCR

Target	**Catalogue#**
Ccl2	Mm00441242_m1
Ccr1	Mm00438260_s1
Ccr2	Mm99999051_gH

Ccr5	Mm01963251_s1
Col1a2	Mm00483888_m1
Col3a1	Mm01254476_m1
Csf1	Mm00432686_m1
Cx3cl1	Mm00436454_m1
Cxcl1	Mm04207460_m1
Cxcl2	Mm00436450_m1
Cxcl12	Mm00445553_m1
Cx3cr1	Mm02620111_s1
Cxcr2	Mm99999117_s1
Cxcr4	Mm01292123_m1
Gapdh	Mm99999915_g1
Icam1	Mm00516023_m1
Icam2	Mm00494862_m1
Il1b	Mm00434228_m1
Il6	Mm00446190_m1
Itga4	Mm01277951_m1
Itgal	Mm00801807_m1
Itgam	Mm00434455_m1
Itgb1	Mm01253230_m1
Itgb2	Mm00434513_m1
Mmp3	Mm00440295_m1
Mmp9	Mm00442991_m1

Mmp10	Mm01168399_m1
Pecam1	Mm01242576_m1
Sele	Mm00441278_m1
Sell	Mm00441291_m1
Selp	Mm01295931_m1
Selplg	Mm01204601_m1
Tgfb1	Mm01178820_m1
Tnf	Mm00443258_m1
Vcam1	Mm01320970_m1

Table 5: Cycle conditions for gene expression qPCR

Step	Temperature	Duration
Initial denaturation	95° C	20 s
Denaturation	95° C	1 s
Annealing/Extension	60° C	20 s

2.2 Cell culture

2.2.1 Generation of bone marrow derived macrophages (BMDM)

Bone marrow cells were isolated from C57BL/6 J mice by flushing the femurs with Roswell Park Memorial Institute (RPMI) 1640 (A1049101, Thermo Fisher Scientific) medium containing 2% of fetal bovine serum (FBS; S0615, Sigma Aldrich). To eliminate erythrocytes, the cell suspension was incubated with 1X RBC Lysis Buffer. After centrifugation, cells were cultured for the indicated time in a medium composed of RPMI 1640, 10% FBS, 100 U/ml penicillin-streptomycin (15140122, Thermo Fisher Scientific) and 50 ng/ml recombinant mouse macrophage colony-stimulating factor (M-CSF) (R&D

Systems, Minneapolis, MN, USA) in 6-well plates (80,000 cells/cm²) in a humidified incubator with 5% CO_2 at 37 °C. Fresh medium was added every day. Every third day, the medium was partially replaced with fresh medium containing the resuspended non-adherent cells.

2.2.2 Application of colchicine

Colchicine was dissolved in the previously described cell culture medium at a final concentration of 0, 1, or 10 ng/ml and daily applied to the cells at the respective time points.

2.2.3 Macrophage precursor differentiation

To identify a possible influence on the differentiation of monocytes to macrophages, BMDM were cultured immediately after seeding with vehicle or colchicine (1 and 10 ng/ml) for a total of 6 days, as shown in **Figure 8.** The number of mature macrophages was determined by flow cytometry using the surface marker F4/80.

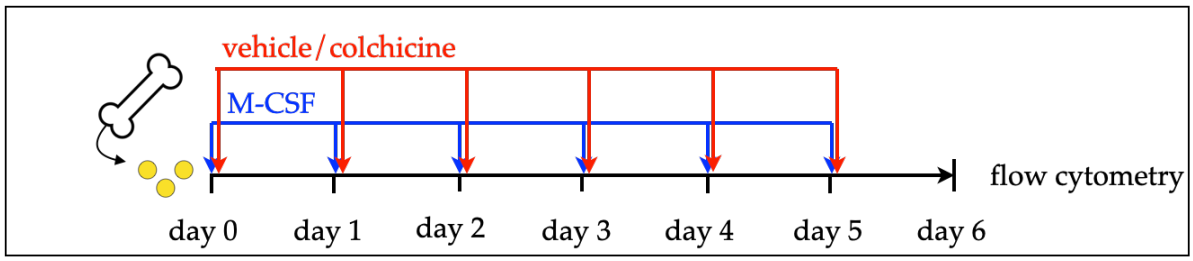

Figure 8: Experimental scheme for precursor differentiation into macrophages

Bone marrow cells were retrieved from one femur and cultured with M-CSF (macrophage colony-stimulating factor) for 6 days to generate bone marrow derived macrophages (BMDM). Either vehicle or colchicine was added once every 24 h starting immediately after seeding. Reprinted under the terms of the Creative Commons CC BY license: Figure 5A from reference (Meyer-Lindemann *et al., 2022).*

2.2.4 Macrophage proliferation

For proliferation experiments, a BrdU staining was used as described in the section Flow cytometric visualization of proliferating cells. Firstly, bone marrow cells were differentiated into macrophages in 100 mm dishes for two or three days as described above and then reseeded in 6-well plates (80,000 cells/cm²). Colchicine (0, 1, or 10 ng/ml final concentration) was added along with fresh culture medium for the last 24 or 48 hours. Two hours before harvesting cells, the BrdU solution (10 µM final concentration, BrdU

Flow Kit, BD Biosciences) was applied. The experimental set-up is shown in **Figure 9.** Subsequently, the non-adherent cells were transferred to a FACS tube. To detach the adherent cells, they were first washed with 2-(4-(2-Hydroxyethyl)-1-piperazinyl)-ethansulfonsäure-(HEPES) buffered saline solution (Promocell, Heidelberg, Germany) and then incubated with Accutase (Sigma Aldrich). The adherent cells were combined with the non-adherent cells and then stained and analyzed by flow cytometry.

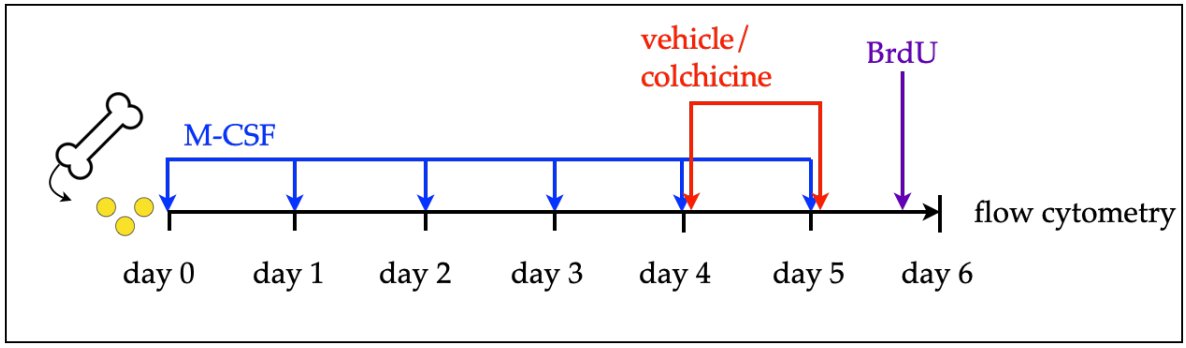

Figure 9: Experimental scheme for macrophage proliferation

Bone marrow cells were retrieved from one femur and cultured with M-CSF (macrophage colony-stimulating factor) for 6 days to generate bone marrow derived macrophages (BMDM). Either vehicle or colchicine was added once every 24 h starting 4 d after seeding. BrdU (bromodeoxyuridine) was administered 2 h before the harvest (day 6 after seeding). Reprinted under the terms of the Creative Commons CC BY license: Figure 5D from reference (Meyer-Lindemann *et al., 2022).*

2.3 Statistical analysis

All statistical analysis was performed using GraphPad Prism version 9. Normality distribution was tested by the D'Agostino-Pearson omnibus K2 normality test or the Shapiro-Wilk test for sample sizes n<8. Two-group comparisons were conducted using two-sided Student´s *t*-test (normally distributed data; Welch's *t*-test was used if variances between both groups were significantly different, as tested by *F*-test) or two-sided Mann-Whitney *U*-test (non-normally distributed data). Comparisons of three or more groups were analyzed using repeated measures one-way ANOVA followed by Dunnett's multiple comparisons test (normally distributed data) and Friedman test followed by Dunn's multiple comparisons test (non-normally distributed data). A two-sided ROUT´s test was used to determine statistical outliers. All graphs present data as mean + standard

error of mean (s.e.m.). Statistical significance was assumed if *P*-values were <0.05. Mouse experiments were conducted at least twice or with n ≥ 10. Where appropriate, variation between experiments was adjusted by normalizing absolute values to a representative experiment.

3 Results

To investigate how anti-inflammatory colchicine beneficially alters the progression of atherosclerosis, atherosclerotic mice (*Apoe*$^{-/-}$ mice on a high cholesterol diet (HCD) for eight weeks) were treated with daily intraperitoneal injections of either vehicle or colchicine (0.25 mg/kg bodyweight) for 4 weeks. The two experimental groups did not differ with respect to total body weight and total LDL cholesterol levels as presented in **Figure 10**.

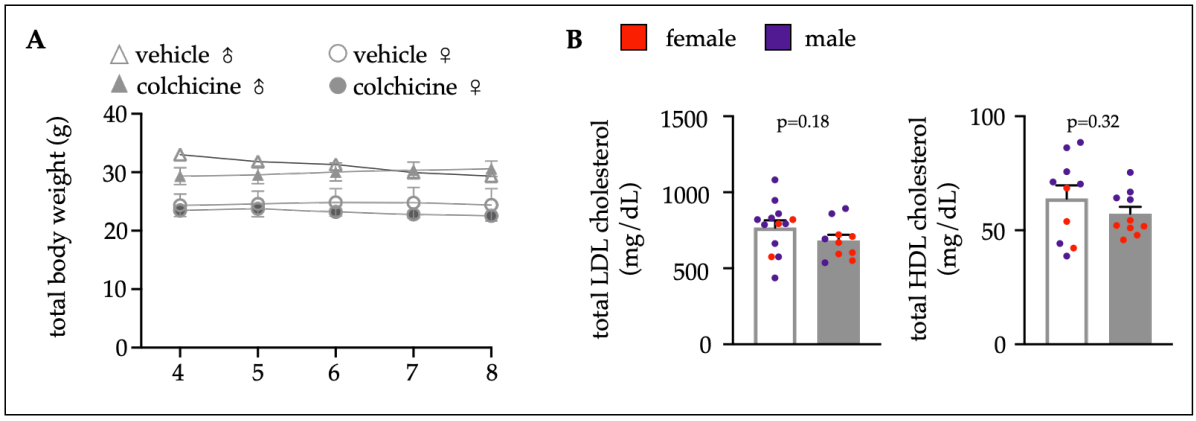

Figure 10: Body weight and lipid levels did not differ between vehicle and colchicine group

Quantification of **(A)** weight development within the treatment period (x-axis indicates time course between weeks 4 and 8 of treatment; *n*=4-6 per group, two-way ANOVA with Dunnett's multiple comparisons test – adjusted *P*-value >0.15 for all comparisons), **(B)** plasma LDL (low-density lipoprotein) cholesterol and HDL (high-density lipoprotein) cholesterol levels in vehicle- vs. colchicine-treated *Apoe*$^{-/-}$ mice (*n*=10 per group, 40-60% female, Student's *t*-test). Data are presented as mean+s.e.m. Dots within bars show the gender of the mice with a color code: purple (male) and red (female). Reprinted under the terms of the Creative Commons CC BY license: Supplementary Figure 2A+B from reference *(*Meyer-Lindemann *et al., 2022).*

3.1 Vascular inflammation: flow cytometric assessment in aortas

First, it was investigated whether colchicine treatment leads to quantitative changes in leukocytes. By performing flow cytometry, leukocyte numbers in aortic plaques were assessed. Here, it was revealed that colchicine treatment decreases the number of inflammatory leukocytes (macrophages, Ly6C^{high} monocytes, and neutrophils) within atherosclerotic aortas compared with vehicle, as portrayed in **Figure 11**.

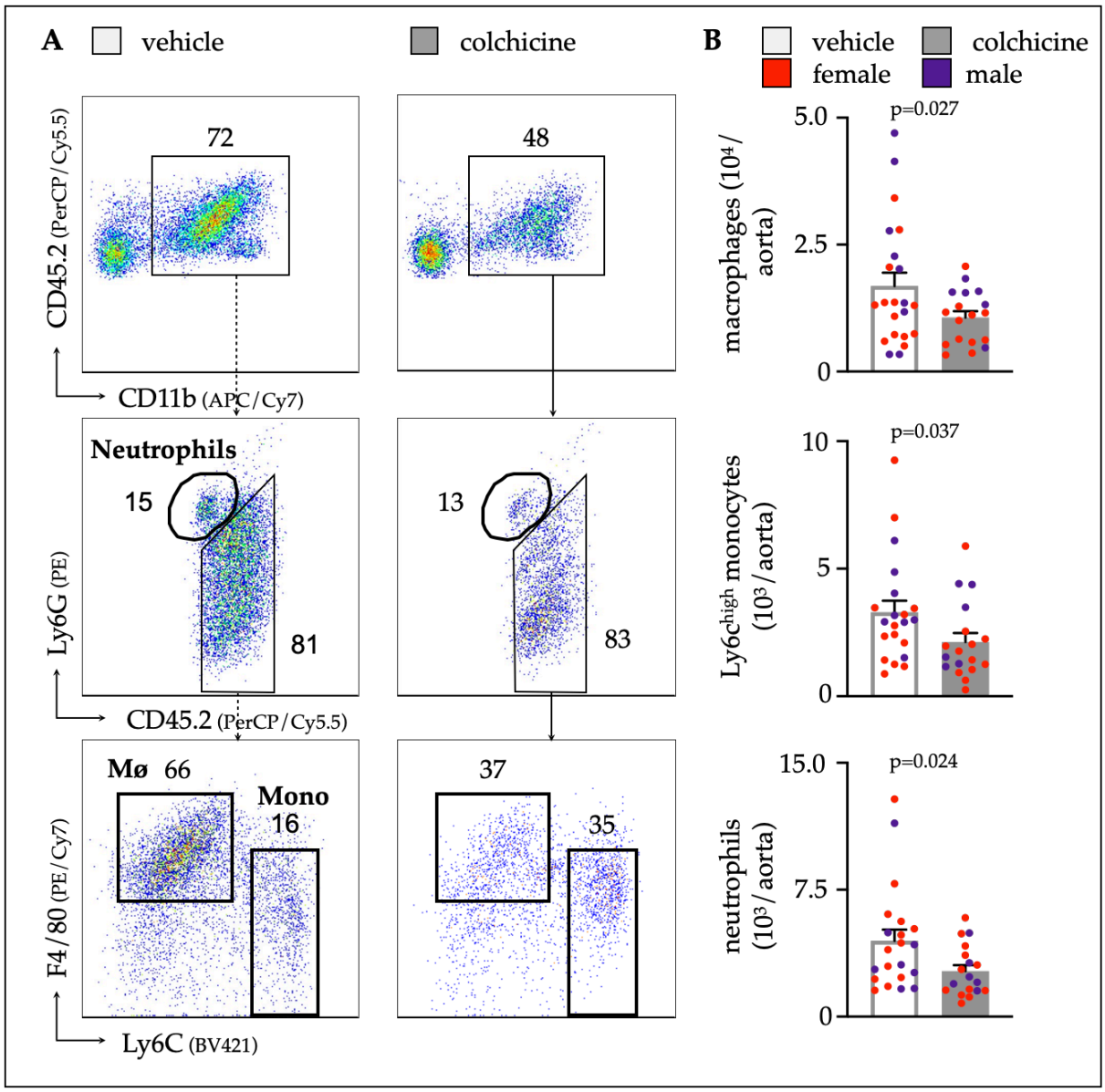

Figure 11: Colchicine reduces plaque inflammation (flow cytometry)

(A) Flow cytometric gating and **(B)** quantification of myeloid cells in atherosclerotic aortas in vehicle- vs. colchicine-treated *Apoe*$^{-/-}$ mice (*n*=18-21 per group, 62-67% female, Welch's *t*-test for macrophages (Mø), Mann-Whitney *U*-test for monocytes (Mono) and neutrophils as appropriate). Numbers next to gates indicate population frequencies (%). Dots within bars show the gender of the mice with a color code: purple (male) and red (female). Reprinted under the terms of the Creative Commons CC BY license: Figure 1A+B from reference (Meyer-Lindemann *et al., 2022).*

3.2 Plaque formation and vascular inflammation: histology of aortic root

To corroborate the flow cytometry results, immunohistochemistry staining was used to quantify CD11b⁺ and Ly6G⁺ cells. CD11b is a myeloid cell (monocytes, macrophages, and neutrophils) marker, whereas Ly6G is mainly located on the surface of neutrophils. In concordance with the results revealed by flow cytometry, a reduction of both CD11b⁺ and Ly6G⁺ cells in aortic plaques was observed, which is demonstrated in **Figure 12**.

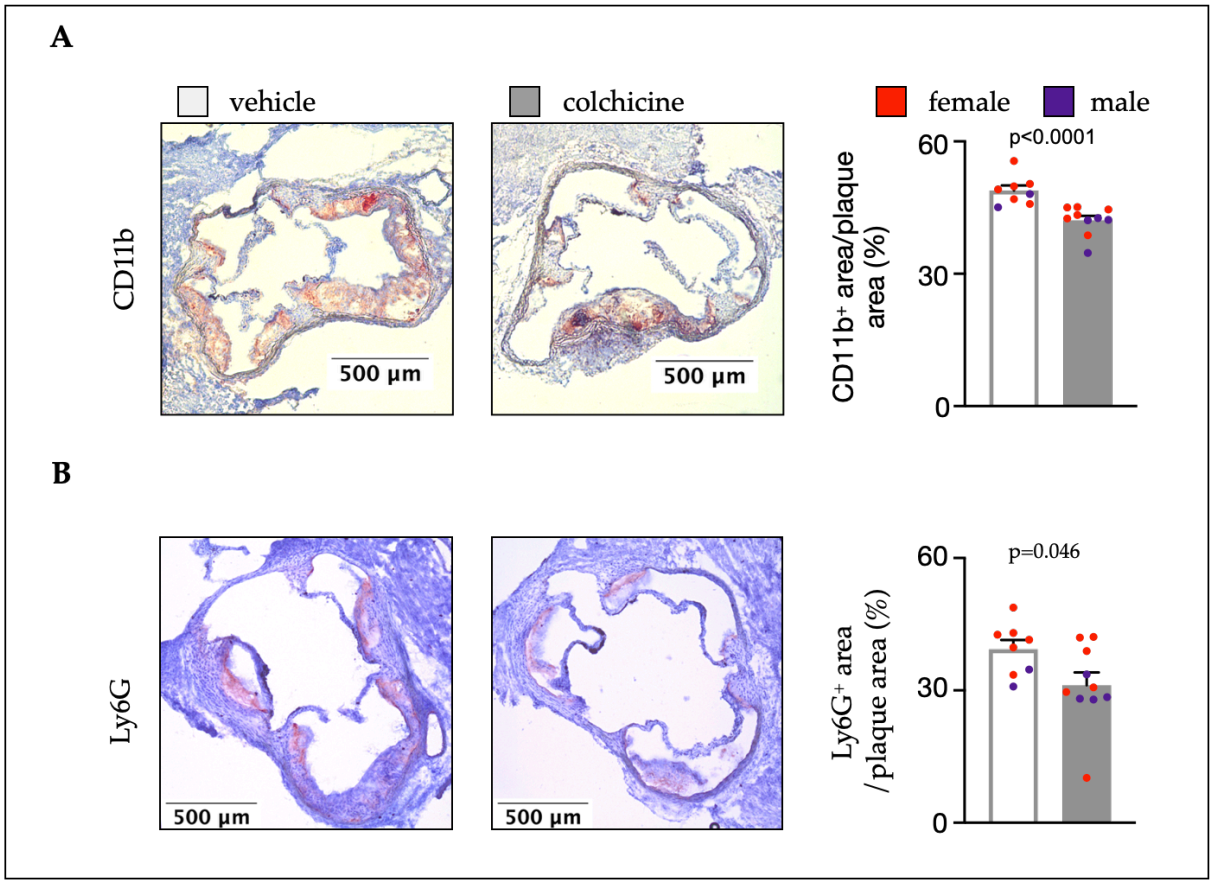

Figure 12: Colchicine mitigates plaque inflammation

Representative immunohistochemical staining for **(A)** myeloid cells (CD11b) and **(B)** neutrophils (Ly6G) of sectioned aortic roots from vehicle- vs. colchicine-treated *Apoe*$^{-/-}$ mice (n=8-10 per group, 60-75% female, Mann-Whitney *U*-test for CD11b, Student's *t*-test for Ly6G). Bar graphs show quantification of positive CD11b- and Ly6G-area, respectively. Scale bars represent 500 µm. Dots within bars show the gender of the mice with a color code: purple (male) and red (female). Reprinted under the terms of the Creative Commons CC BY license: Figure 1C+D from reference (Meyer-Lindemann *et al., 2022*).

3.3 Further characterization of the plaque: size and composition

Next, the overall plaque character was characterized using histology and qPCR. By performing Masson Trichrome staining in aortic root sections, a smaller plaque size was detected in mice treated with colchicine as displayed in **Figure 13**.

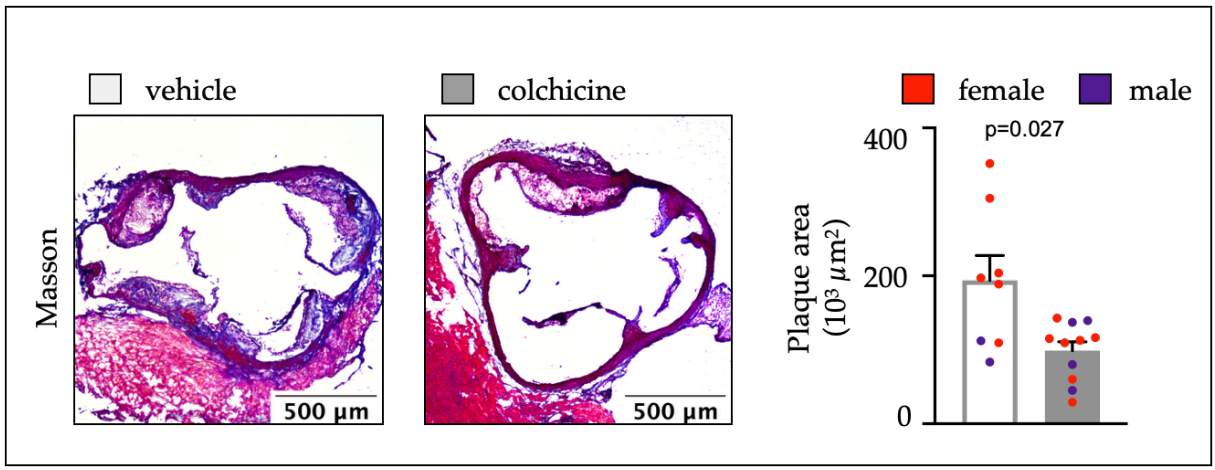

Figure 13: Colchicine decreases atherosclerotic plaque size

Representative Masson Trichrome staining and quantification of total plaque area (*n*=8-11 per group, 64-75% female, Welch's *t*-test). Scale bars represent 500 µm. Dots within bars show the gender of the mice with a color code: purple (male) and red (female). Reprinted under the terms of the Creative Commons CC BY license: Figure 1F from reference (Meyer-Lindemann *et al., 2022).*

By qPCR, the composition of aortic plaques was assessed and the expression of different genes in the aortic arch was analyzed. Specifically, changes in gene expression affecting vascular integrity, cytokines, growth factors, and chemokines were found. To uncover changes in vascular architecture, the gene expression of matrix metalloproteinases (MMPs) and collagenases was examined as portrayed in **Figure 14.** Here, a colchicine-mediated decreased expression of *MMP-3*, *MMP-9* and *MMP-10* was detected. The genetic expression level of collagenases remained unchanged. Further, it was tested whether cytokines and growth factors are modulated by colchicine. It was found that *CSF-1* and tumor necrosis factor (*TNF)* were significantly downregulated by colchicine. The expression of other investigated key players in inflammation, *Il-1ß* and *Il-6*, was not changed by colchicine. Levels of transforming growth factor beta 1 (*TGFβ1)* remained

unaltered as well. Next, it was examined whether chemokines were affected by colchicine. However, apart from an increased expression of C-X-C motif-chemokine ligand 12 (*CXCL12*), a chemoattractant for lymphocytes, there was no difference regarding levels of CC motif chemokine ligand 2 (*CCL-2*), C-X-C motif chemokine ligand 1 (*CXCL-1*), C-X-C motif chemokine ligand 2 (*CXCL-2*), and C-X3-C motif chemokine ligand 1 (*CX3CL1*).

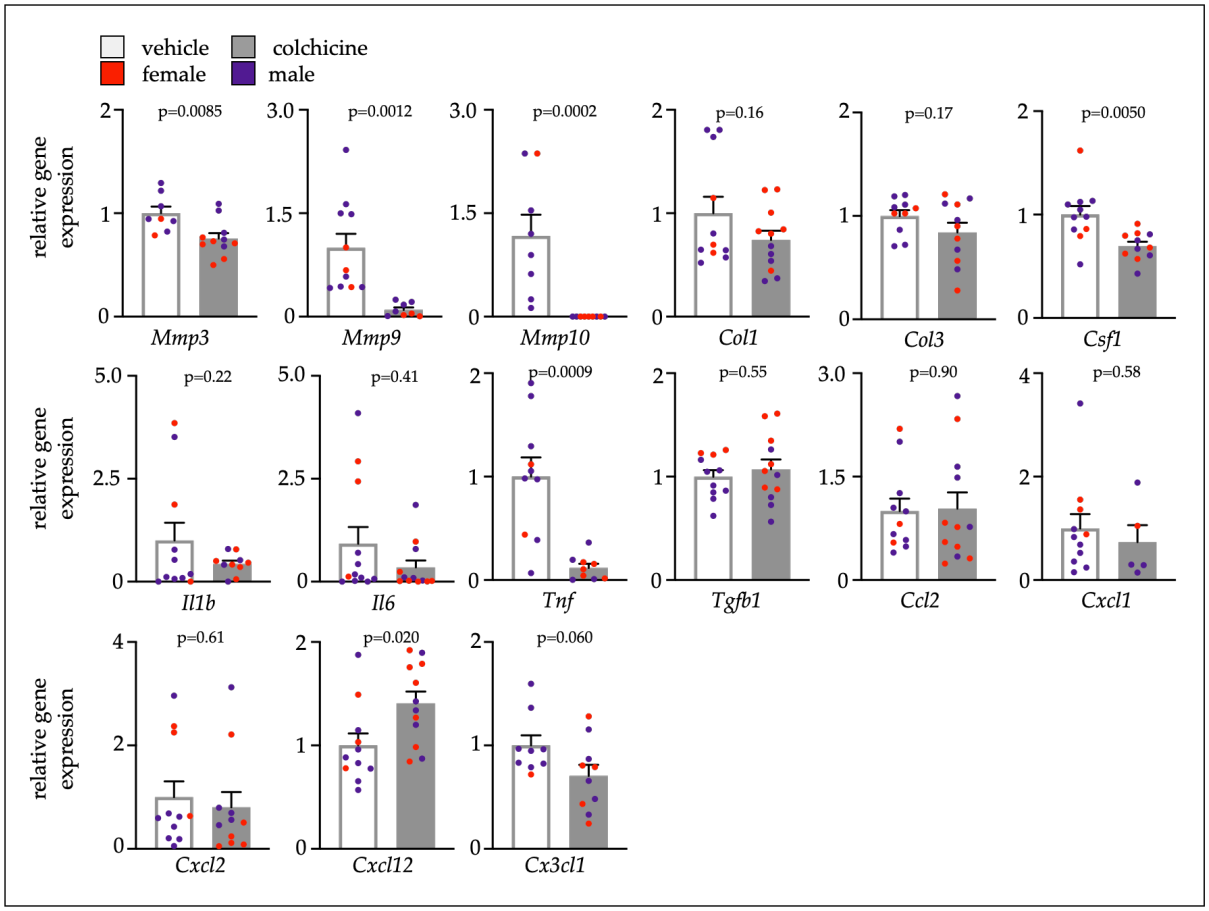

Figure 14: Colchicine reduces expression of inflammation-related factors

Quantitative real-time PCR for gene expression quantification of fibrotic, inflammatory and cytokine genes in aortas of vehicle- vs. colchicine-treated *Apoe*$^{-/-}$ mice (*n*=5-12 per group, 55-88% female, Student's/Welch's *t*-test or Mann-Whitney *U*-test as appropriate). *Mmp3*/*Mmp9*/*Mmp10* (matrix metalloproteinase-3/9/10), *Col1*/*Col3* (collagen-1/3), *Csf1* (colony stimulating factor 1), *Il1β* (interleukin 1 beta), *Il6* (interleukin 6), *Tnf* (tumor necrosis factor), *Tgfb1* (transforming growth factor beta 1), *Ccl2* (C-C motif chemokine ligand 2), *Cxcl1* (C-X-C motif chemokine ligand 1), *Cxcl2* (C-X-C motif chemokine ligand 2), *Cxcl12* (C-X-C motif chemokine ligand 12), *Cx3cl1* (C-X3-C motif chemokine ligand 1). Data are presented as mean + s.e.m. Dots within bars show the gender of the mice with a color code: purple (male) and red (female). Reprinted under the terms of the Creative Commons CC BY license: Figure 1E from reference (Meyer-Lindemann *et al., 2022)*

Deducing from these results, colchicine leads to quantitative changes in inflammatory cells. The accumulation of leukocytes in aortic plaques is decreased which results in a less inflammatory phenotype. Thus, the next step was to identify how exactly colchicine affects the individual components of the leukocyte supply chain which was previously described in **Figure 2.**

3.4 Effects on leukocyte trafficking

3.4.1 Leukocyte recruitment to aortic plaques

In the first step, it was analyzed whether colchicine affects recruitment, i.e., the uptake of leukocytes into atherosclerotic plaques by performing adoptive transfer experiments. Leukocytes were isolated from naïve transgenic *Ubc-GFP* mice and subsequently transferred into atherosclerotic mice treated with PBS or colchicine for 4 weeks. Twenty-four hours later, GFP^{high} leukocytes incorporated into aortic plaques were tracked. As shown in **Figure 15**, mice exposed to colchicine showed a decreased uptake of GFP^{high} leukocytes. Hence, colchicine diminishes the recruitment of leukocytes.

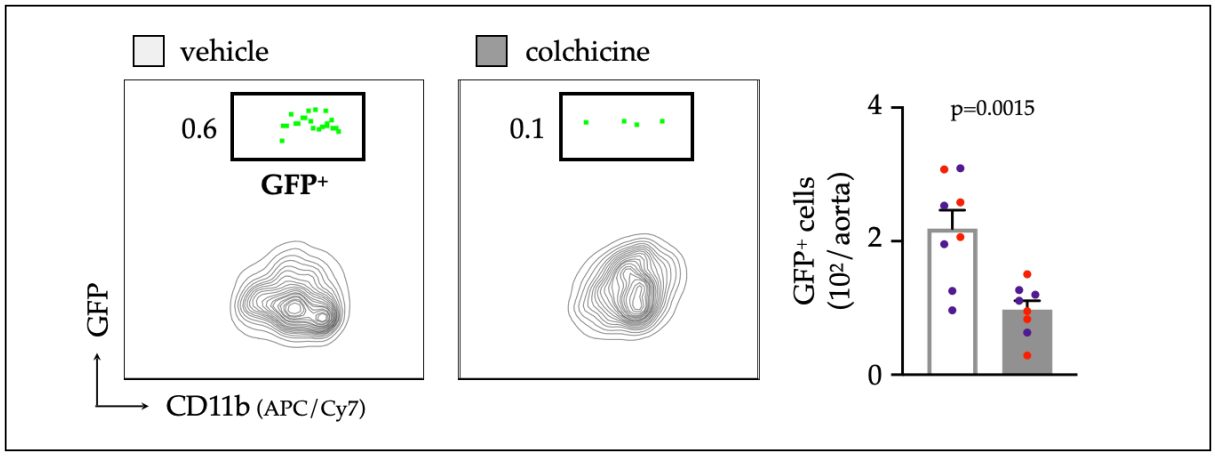

Figure 15: Colchicine treatment decreases recruitment into atherosclerotic aortas

Flow cytometric gating and quantification of GFP^{high} (GFP^{+}) myeloid cells in atherosclerotic aortas 24 h after adoptive transfer of GFP^{high} monocytes and neutrophils into vehicle- vs. colchicine-treated *Apoe*$^{-/-}$ mice (n=8 per group, 38-50% female, Student's t-test). Dots within bars show the gender of the mice with a color code: purple (male) and red (female). Reprinted under the terms of the Creative Commons CC BY license: Figure 2A from reference (Meyer-Lindemann *et al., 2022)*

Subsequently, it was investigated how exactly colchicine reduces leukocyte recruitment. Recruitment is a complex interplay with two main players: ECs, which act as a barrier layer lining the inside of the vessel wall, and leukocytes, which circulate in the blood. To find out which cells are affected by colchicine, ECs and leukocytes, particularly Ly6C^{high} monocytes and neutrophils, were obtained by flow cytometry. Next, the genetic expression of their adhesion molecules, integrins, and chemokines was analyzed.

3.4.1.1 Endothelial Cells

The effect of colchicine on ECs is summarized in **Figure 16**. Regarding the quantification of mean-fluorescent intensities (MFI) representing relative protein levels, no colchicine-driven alterations on EC adhesion molecules were observed **(A+B+C)**. In line, the relative expression of the genes encoding for intercellular adhesion molecule 1 (*ICAM-1*), intercellular adhesion molecule 2 (*ICAM-2*), vascular cell adhesion protein 1 (*VCAM-1*), E-selectin, and P-selectin showed no differences between both groups. The assessment of chemokines revealed that *CCL2* and *CX3CL1* – both of which proteins are chemotactic for monocytes – were decreased in the colchicine group, while the level of *CXCL2* was elevated **(D).**

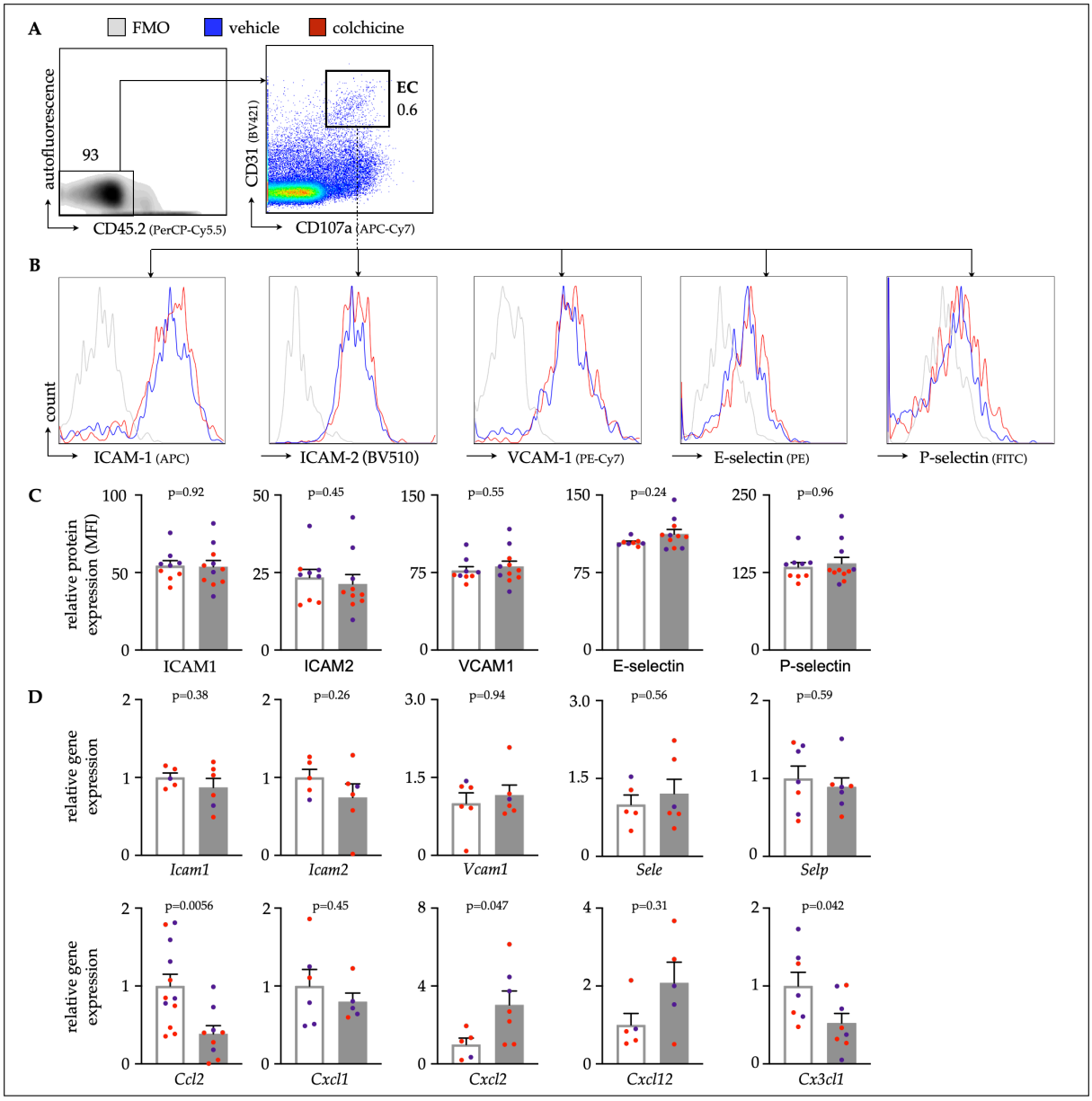

Figure 16: Colchicine treatment affects endothelial cells marginally

Gating strategy **(A)** and **(B)** histograms of leukocyte adhesion molecules on aortic endothelial cells (EC) from vehicle- vs. colchicine-treated *Apoe*$^{-/-}$ mice. **(C)** Quantification of mean fluorescent intensities (MFI, representing relative protein levels) of adhesion molecules expressed by aortic ECs from vehicle- vs. colchicine-treated *Apoe*$^{-/-}$ mice (*n*=9-11 per group, 44-55% female, Student's *t*-test or Mann-Whitney *U*-test as appropriate). Bar graphs indicate the relative change of MFI as standardized to controls. FMO (fluorescence minus one (respective antibody omitted)) control. **(D)** Quantitative real-time PCR for gene expression quantification in fluorescence-activated cell sorting (FACS)-purified aortic ECs of vehicle- vs. colchicine-treated *Apoe*$^{-/-}$ mice (*n*=3-12 per group, 33-83% female, Student's/ Welch's *t*-test or Mann-Whitney *U*-test, as appropriate). Abbreviations: ICAM-1/ *Icam1* (intercellular adhesion molecule 1), ICAM-2/ *Icam2* (intercellular adhesion molecule 2), VCAM-1/ *Vcam1* (vascular cell adhesion protein 1), E-selectin/ *Sele*, P-selectin/ *Selp*, L-selectin/ *Sell*, selectin P ligand/ *Selplg*, platelet endothelial cell adhesion molecule-1/ *Pecam1*, C-C motif chemokine ligand 2/ *Ccl2*, C-X-C motif chemokine ligands 1+2+12/ *Cxcl1*/ *Cxcl2*/ *Cxcl12*, C-X3-C motif ligand 1/ *Cx3cl1*. Data are presented as mean + s.e.m. Numbers next to gates indicate

population frequencies (%). Dots within bars show the gender of the mice with a color code: purple (male) and red (female). Reprinted under the terms of the Creative Commons CC BY license: Figure 2B+C+D from reference *(*Meyer-Lindemann *et al., 2022)*

3.4.1.2 Leukocytes

As shown in **Figure 17,** the expression of leukocyte adhesion molecules was partially altered by colchicine. In monocytes **(B)**, Platelet and Endothelial Cell Adhesion Molecule 1 (*PECAM1)* was down-regulated by colchicine, while in neutrophils **(A)** the expression of *L-Selectin* was decreased. Further, colchicine induced profound changes in the expression of integrins. The data revealed that colchicine downregulates integrin subunit alpha L (*ITGAL)*, the alpha unit of lymphocyte function-associated antigen 1 (*LFA-1*), in both monocytes and neutrophils. Further, the integrin subunit alpha 4 (*ITGA4)* and the integrin subunit beta 1 (*ITGB1)*, which together form integrin alpha 4 beta 1 (*VLA4*), were decreased in monocytes. The integrin subunit alpha M *(ITGAM)* was upregulated in monocytes by colchicine. Additionally, the expression of chemokine receptors was strongly altered by colchicine. In monocytes, C-C chemokine receptor types 5 (*CCR5),* C-X-C motif chemokine receptor type 2 (*CXCR2)*, C-X-C motif chemokine receptor type 4 (*CXCR4)*, as well as C-X3-C motif chemokine receptor 1 (*CX3CR1)* were decreased by colchicine. In neutrophils, *CXCR4* was depleted while C-C chemokine receptor type 1 (*CCR1)* was upregulated.

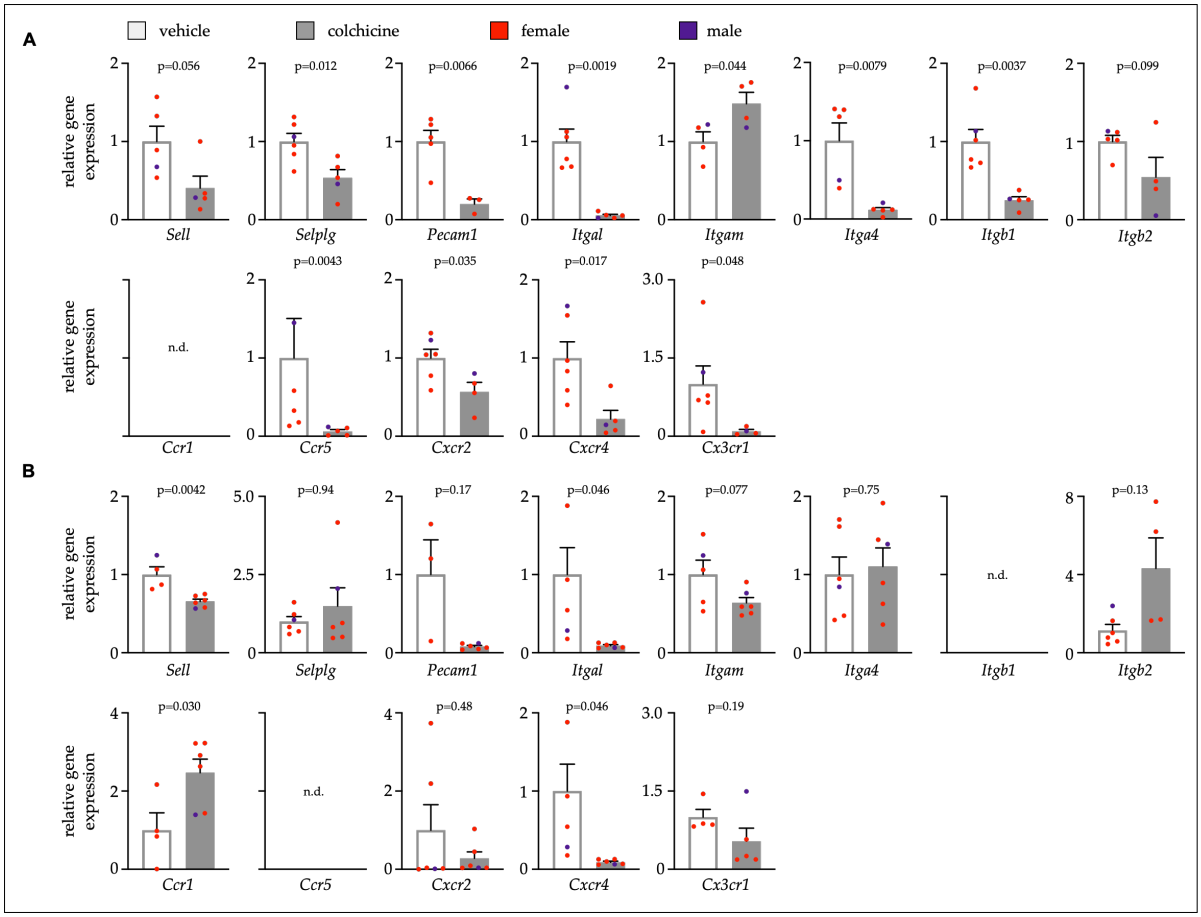

Figure 17: Colchicine treatment silences neutrophil and monocyte activation

Quantitative real-time PCR for gene expression quantification in fluorescence-activated cell sorting (FACS)-purified **(A)** blood neutrophils and **(B)** blood Ly6C^{high} monocytes of vehicle- vs. colchicine-treated *Apoe*$^{-/-}$ mice (*n*=3-12 per group, 33-83% female, Student's/ Welch's *t*-test or Mann-Whitney *U*-test as appropriate). Abbreviations: L-selectin/ *Sell*, selectin P ligand/ *Selplg*, platelet endothelial cell adhesion molecule-1/ *Pecam1*, integrin subunit alpha L/ *Itgal*, integrin subunit alpha M/ *Itgam*, integrin subunit alpha 4/ *Itga4*, integrin subunit beta 1/ *Itgb1*, integrin subunit beta 2/ *Itgb2*, C-C chemokine receptor types 1+5/ *Ccr1*/ *Ccr5*, C-X-C motif chemokine receptor types 2+4/ *Cxcr2*/ *Cxcr4*, and C-X3-C motif chemokine receptor 1/ *Cx3cr1*. Data are presented as mean + s.e.m. Numbers next to gates indicate population frequencies (%). Dots within bars show the gender of the mice with a color code: purple (male) and red (female). Reprinted under the terms of the Creative Commons CC BY license: Figure 2E+F from reference (Meyer-Lindemann *et al., 2022)*

These results indicate that the colchicine-induced decrease in uptake of inflammatory cells into the plaque is predominantly caused by altered recruitment capacities of leukocytes. To confirm our findings, an additional experiment was designed. Here, GFP^{high} leukocytes were isolated from *Ubc-GFP* mice that were previously treated with vehicle or colchicine for one week and adoptively transferred into *Apoe*$^{-/-}$ mice. 24 hours later, GFP^{high} leukocytes

incorporated into plaque were assessed. The experimental set-up is described in **Figure 7.** The experiment revealed that the uptake of leukocytes into plaques was diminished if leukocytes were previously exposed to colchicine, which is shown in **Figure 18.**

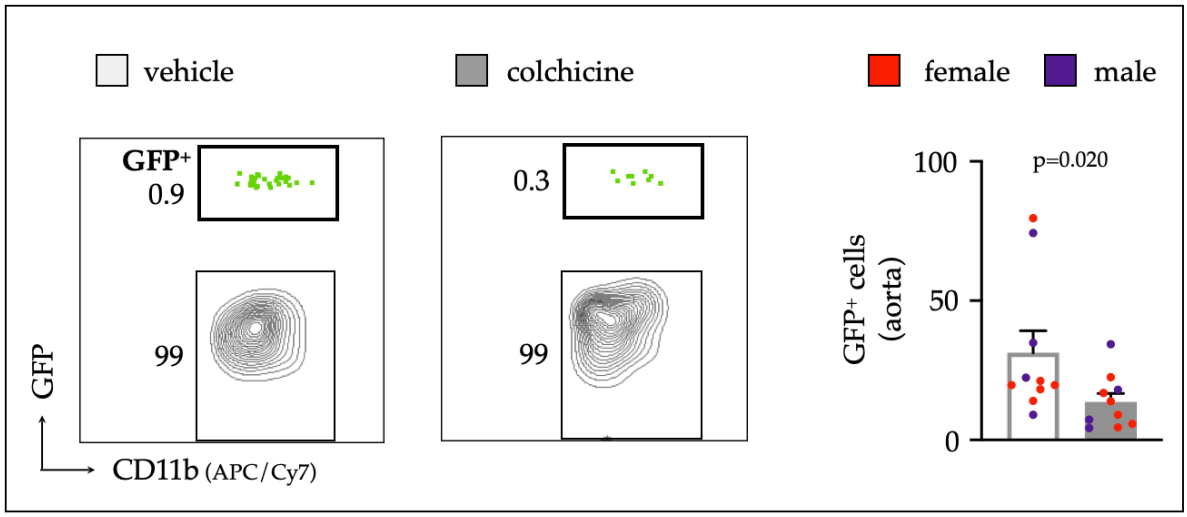

Figure 18: Colchicine-exposed neutrophils and monocytes show reduced recruitment capacities

Flow cytometric gating and quantification of GFP^{high} myeloid cells (GFP^{+}) in atherosclerotic aortas 24 h after adoptive transfer of either vehicle- or colchicine-exposed GFP^{high} monocytes and neutrophils into *Apoe*$^{-/-}$ mice (*n*=10 per group, 60% female, Mann-Whitney *U*-test). Data are presented as mean + s.e.m. Numbers next to gates indicate population frequencies (%). Dots within bars show the gender of the mice with a color code: purple (male) and red (female). Reprinted under the terms of the Creative Commons CC BY license: Figure 3B+C from reference (Meyer-Lindemann *et al., 2022)*

3.4.2 Leukocyte production and release

The next question addressed was whether colchicine affects leukocyte production. Therefore, leukocyte numbers in bone marrow and blood were compared to find out whether colchicine impacts production and/or release of leukocytes. As shown in **Figure 19**, our data revealed no differences in leukocyte counts in either blood **(A+B)** or bone marrow **(C+D)**.

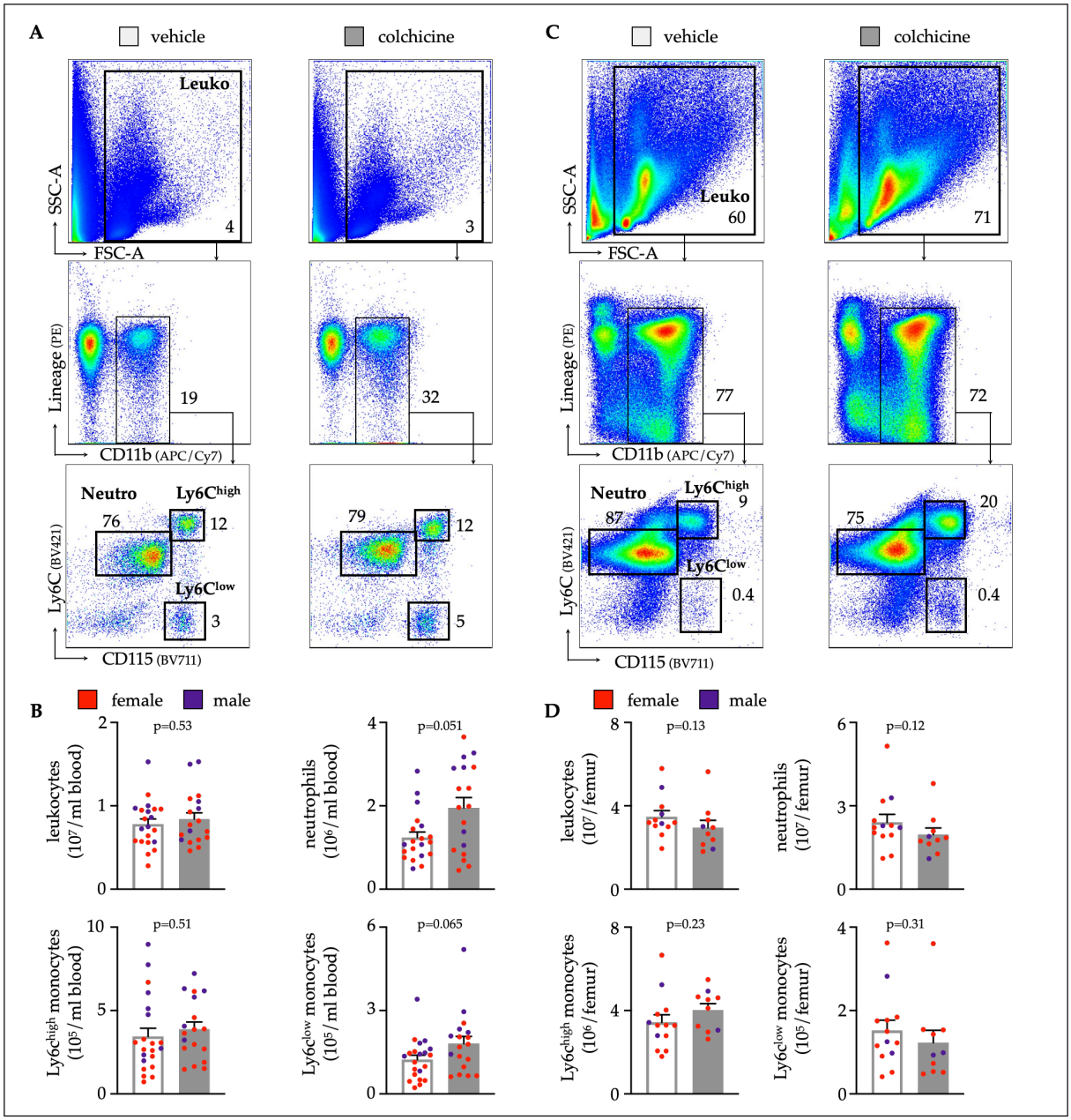

Figure 19: Colchicine treatment does not alter numbers of blood leukocyte subsets

Flow cytometric gating and quantification of myeloid cells in the blood **(A+B)** (*n*=18-21 per group, 62-67% female, Student's *t*-test for total leukocytes and Ly6C^{high} monocytes (Mono^{high}), Mann-Whitney *U*-test for neutrophils (Neu) and Ly6C^{low} monocytes (Mono^{low})) and bone marrow **(C+D)** of vehicle- vs. colchicine-treated *Apoe*$^{-/-}$ mice (*n*=10-13 per group, 77-80% female, Mann-Whitney *U*-test). Data are presented as mean + s.e.m. Numbers inside/ next to gates indicate population frequencies (%). Reprinted under the terms of the Creative Commons CC BY license: Figure 4 from reference (Meyer-Lindemann *et al., 2022)*

3.5 The behavior inside atherosclerotic plaques: macrophage differentiation and proliferation

To fully investigate the components of the leukocyte supply chain, the attention was lastly turned to macrophages. As mentioned in the section Pathogenesis of atherosclerosis, macrophages play a particularly important role as disease driver and modifier in atherosclerosis. Two possible pathways, by which colchicine might act on macrophages, were investigated. On the one hand, macrophage development, i.e., macrophage precursor differentiation was investigated. On the other hand, the impact of colchicine on macrophage proliferation was assessed. The experimental set-up is described in detail in the section Generation of bone marrow derived macrophages (BMDM. To determine the time point at which most monocytes differentiate into macrophages, a timeline was first created. Using flow cytometry, the degree of monocyte maturation based on the surface marker F4/80 was daily assessed. The highest rate of differentiation occurred on days 3-5, which is shown in **Figure 20**.

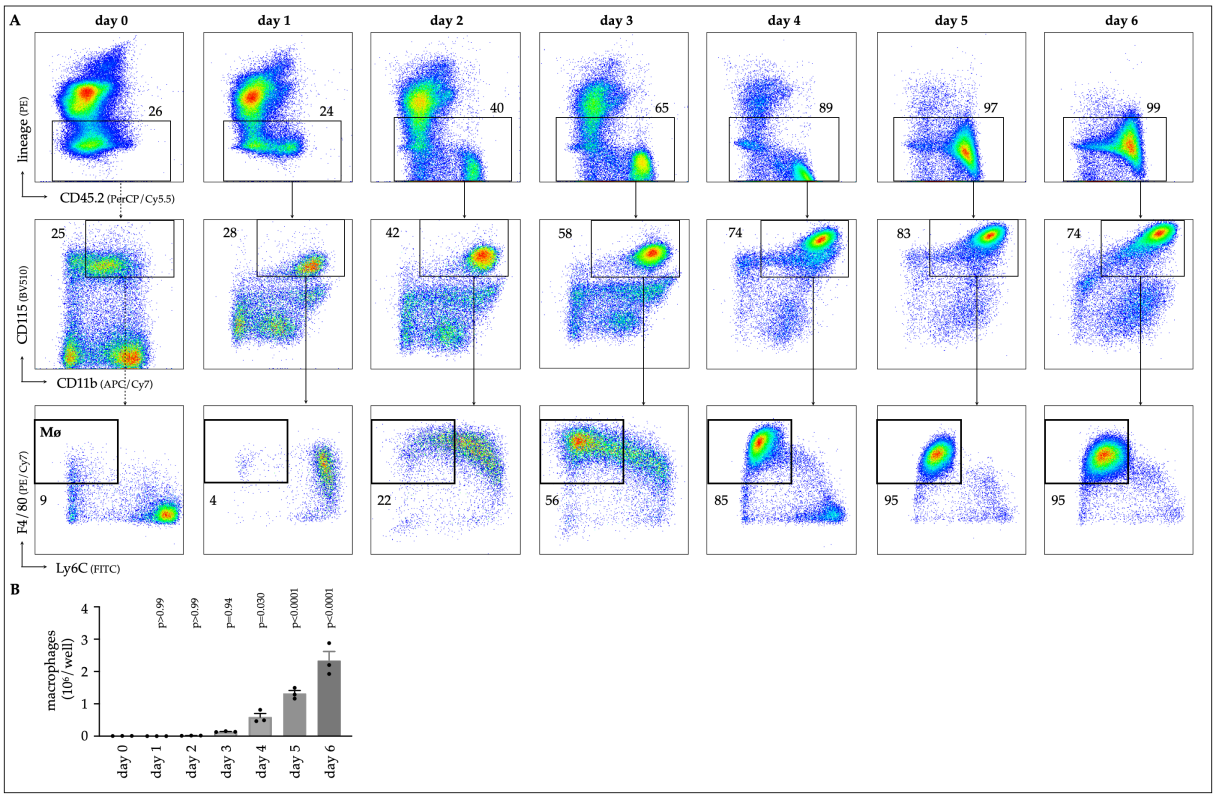

Figure 20: Macrophage numbers rise from day 3 onward in cultured whole bone marrow cells incubated with M-CSF

(A) Experimental scheme for culturing of mouse whole bone marrow cells in the presence of M-CSF (macrophage colony-stimulating factor) to generate bone marrow-derived macrophages (Mø). **(B)** Flow cytometric gating and **(C)** quantification of macrophages in kinetic experiments (*n*=3 per group, each *n* represents one donor animal, repeated measures one-way ANOVA with Dunnett's multiple comparisons test). Data are presented as mean + s.e.m. Numbers next to gates indicate population frequencies (%). Reprinted under the terms of the Creative Commons CC BY license: Supplementary Figure 4 from reference (Meyer-Lindemann *et al., 2022)*

Next, the question of which colchicine dose was most relatable *in vitro* was explored. According to previously described dosages in literature, three different colchicine concentrations (1, 10, 100 ng/ml) were tested. Since the dosage of 100 ng/ml proved to be cytotoxic (as displayed in **Figure 21**) it was decided to proceed with 1 and 10 ng/ml colchicine.

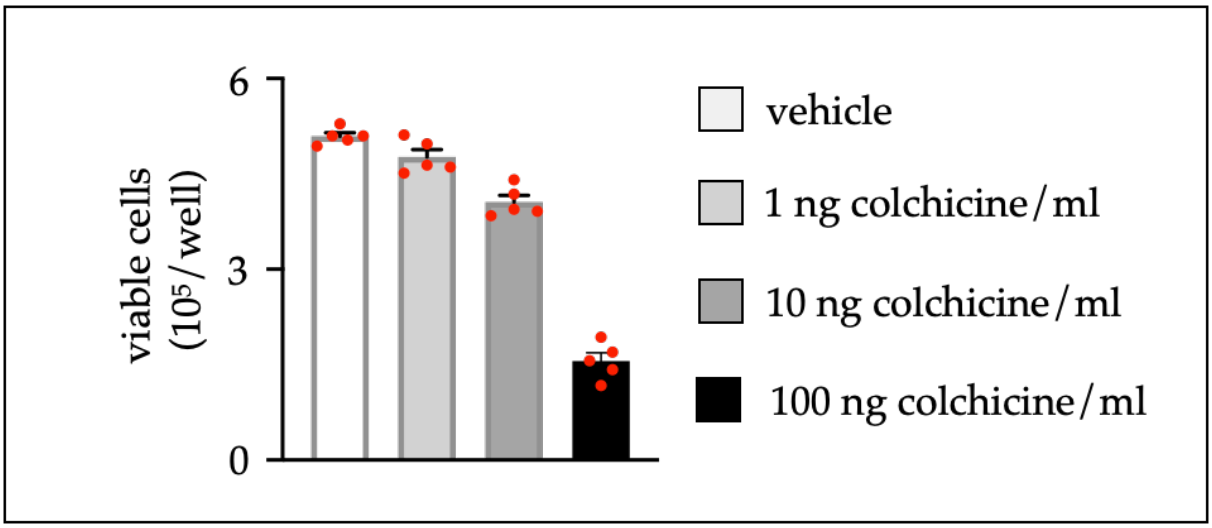

Figure 21: Colchicine concentration test on BMDM cell culture

Quantification of viable cells on day 3 of culture after 48 h of treatment with vehicle (white bar) or different concentrations of colchicine (1, 10, 100 ng/ml, grey scale bars). (*n*=5 per group, each *n* represents one donor animal).

3.5.1 Macrophage precursor differentiation

To identify a possible influence on the differentiation of monocytes to macrophages, BMDM were cultured immediately after seeding with vehicle or colchicine (1 and 10 ng/ml) for a total of 6 days as shown in **Figure 8**. The number of mature macrophages were then quantified using the surface marker F4/80 by flow cytometry. As portrayed in **Figure**

22, the experiment showed no difference between vehicle, 1 ng/ml, and 10 ng/ml of colchicine.

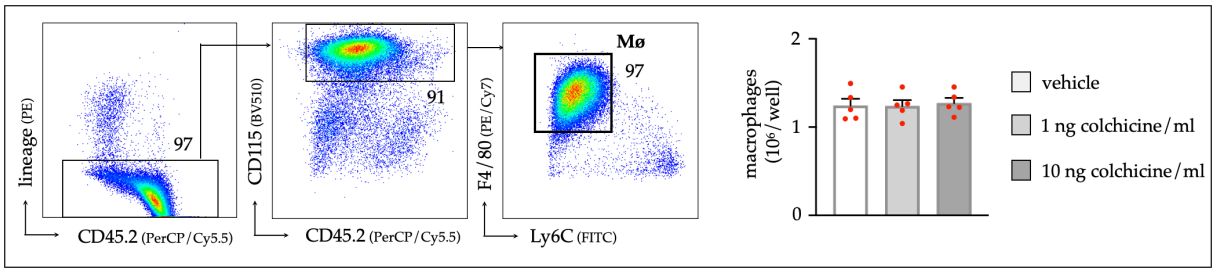

Figure 22: Colchicine treatment does not affect macrophage precursor differentiation after 6 days

Flow cytometric gating and quantification of macrophage (Mø) numbers 6 days after either vehicle or colchicine exposure (*n*=5 per group, each *n* represents one donor animal; repeated measures one-way ANOVA with Dunnett's multiple comparisons test). Reprinted under the terms of the Creative Commons CC BY license: Figure 5B+C from reference *(*Meyer-Lindemann *et al., 2022)*

Nevertheless, to detect a possible influence of colchicine on macrophage differentiation, the experimental setup was extended by additional time points that are represented in **Figure 23**. However, even with modified exposure to M-CSF and vehicle/ colchicine, there was no difference between the groups. Thus, the chosen experimental design shows no evidence regarding an effect of colchicine on macrophage differentiation.

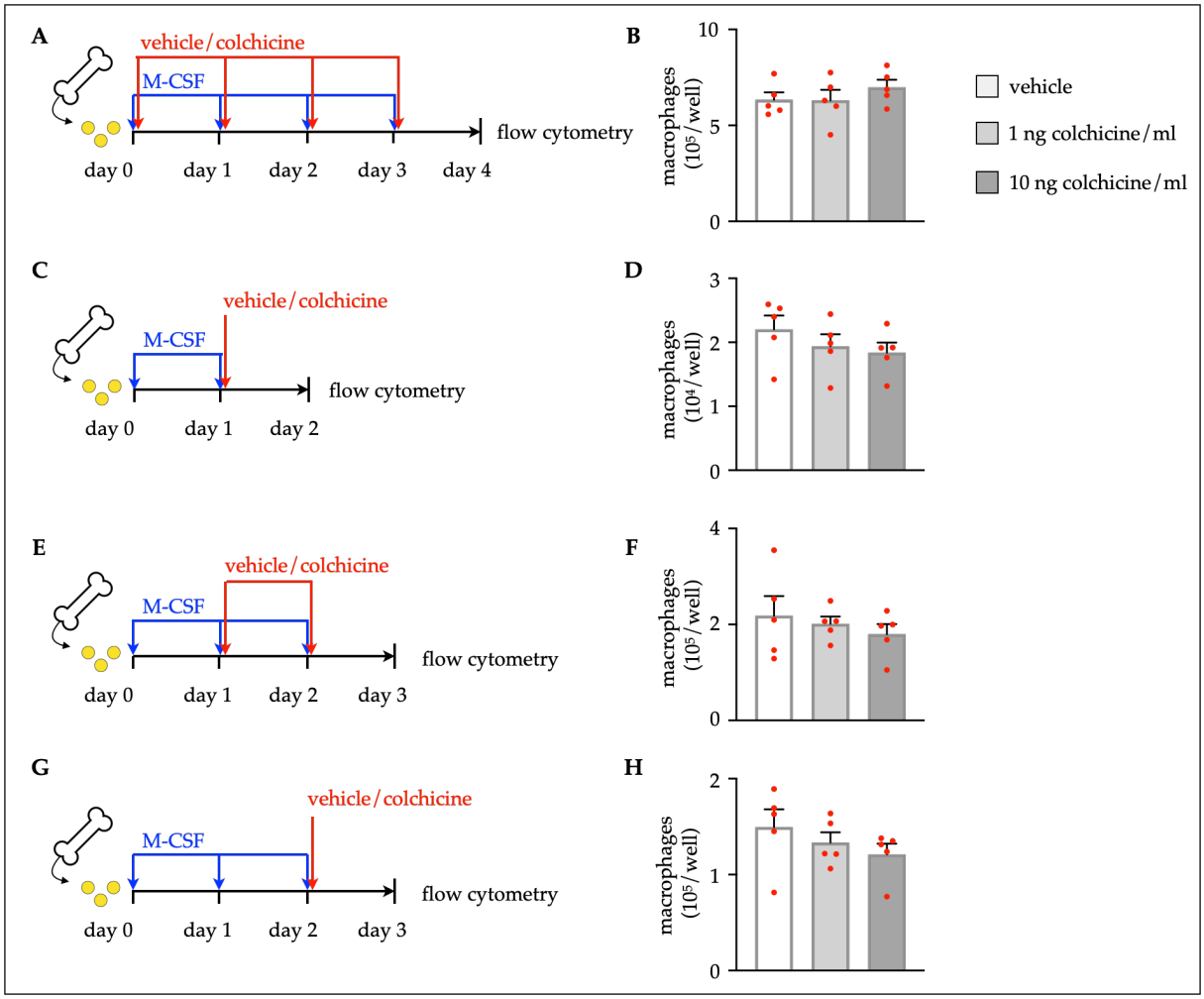

Figure 23: Treatment with colchicine for varying periods of time does not affect the differentiation of macrophage progenitors.

(A,C,E,G) Experimental schemes for precursor differentiation into macrophages. In brief, bone marrow cells were retrieved from one femur and cultured with M-CSF (macrophage colony-stimulating factor) for the indicated time to generate bone marrow-derived macrophages (BMDM). Either vehicle or colchicine was added once every 24 hours as indicated in the Figure. **(B,D,F,H)** Quantification of macrophage numbers after either vehicle or colchicine exposure (*n*=5 per group, each *n* represents one donor animal; repeated measures one-way ANOVA with Dunnett's multiple comparisons test or Friedman test followed by Dunn's multiple comparisons test as appropriate). Data are presented as mean + s.e.m. Reprinted under the terms of the Creative Commons CC BY license: Supplementary Figure 5 from reference (Meyer-Lindemann *et al., 2022)*

3.5.2 Macrophage proliferation

To investigate the influence of colchicine on macrophage proliferation, the cell cycle of macrophages was analyzed by flow cytometry using a BrdU staining. The experimental setup, which is shown in **Figure 9**, was as follows: monocytes were first differentiated into

macrophages by culturing them with M-CSF for 6 days. From day 4, cells were exposed to vehicle/colchicine for 48 h. BrdU was added 2 h before seeding on day 6. The quantification of BrdU⁺ macrophages is displayed in **Figure 24**. As there was no difference between vehicle- and colchicine-exposed groups, it can be concluded that colchicine does not affect macrophage proliferation in this setting.

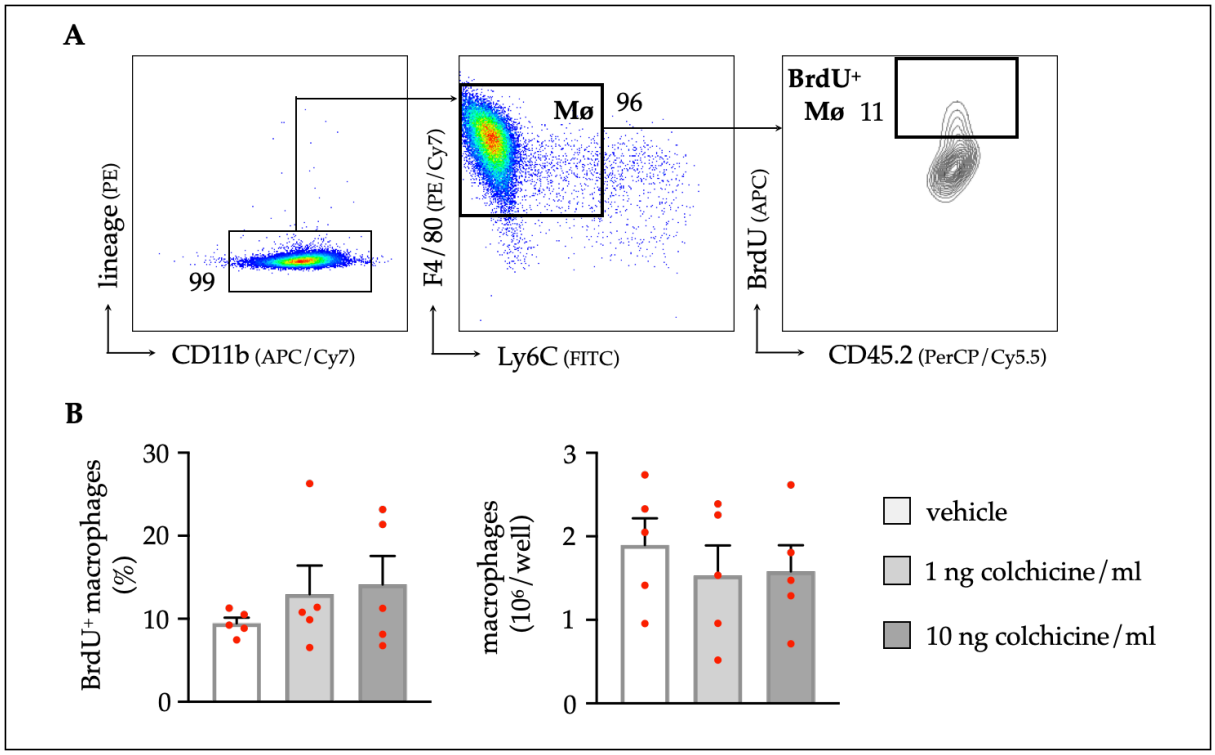

Figure 24: Colchicine treatment does not impact macrophage proliferation

(A) Flow cytometric gating and **(B)** quantification of BrdU⁺ macrophage (BrdU⁺ Mø) frequencies (Friedman test followed by Dunn's multiple comparisons test) and total macrophage numbers 48 h after either vehicle or colchicine exposure (repeated measures one-way ANOVA with Dunnett's multiple comparisons test). *n*=5 per group (each *n* represents one donor animal). Data are presented as mean + s.e.m. Numbers next to gates indicate population frequencies (%). Reprinted under the terms of the Creative Commons CC BY license: Figure 5E+F from reference (Meyer-Lindemann *et al., 2022)*

3.6 Simulation of the Colchicine Cardiovascular Outcomes Trial (COLCOT)

Because myocardial infarction is an accelerator for atherosclerosis progression, the previously mentioned COLCOT trial was simulated in mice to study if colchicine can also exert its beneficial effects in an advanced disease state. The experimental set-up is

portrayed in **Figure 5**. The experiment demonstrates that colchicine treatment decreases the expansion of aortic macrophages, Ly6C^{high} monocytes, and neutrophils, which is shown in **Figure 25 (A+B)**. Because in early disease the atheroprotective mechanism of colchicine consists of decreased recruitment of leukocytes to plaques, it was important to verify whether this also applies to advanced disease. The experimental set-up was extended by adoptively transferring GFP^{high} leukocytes from *Ubc-GFP* donor mice into the infarcted mice one day prior to harvest. Fewer GFP^{high} leukocytes were recruited in the aorta in colchicine treated mice **(C+D).** Thus, colchicine acts in a similar manner in both early and advanced disease.

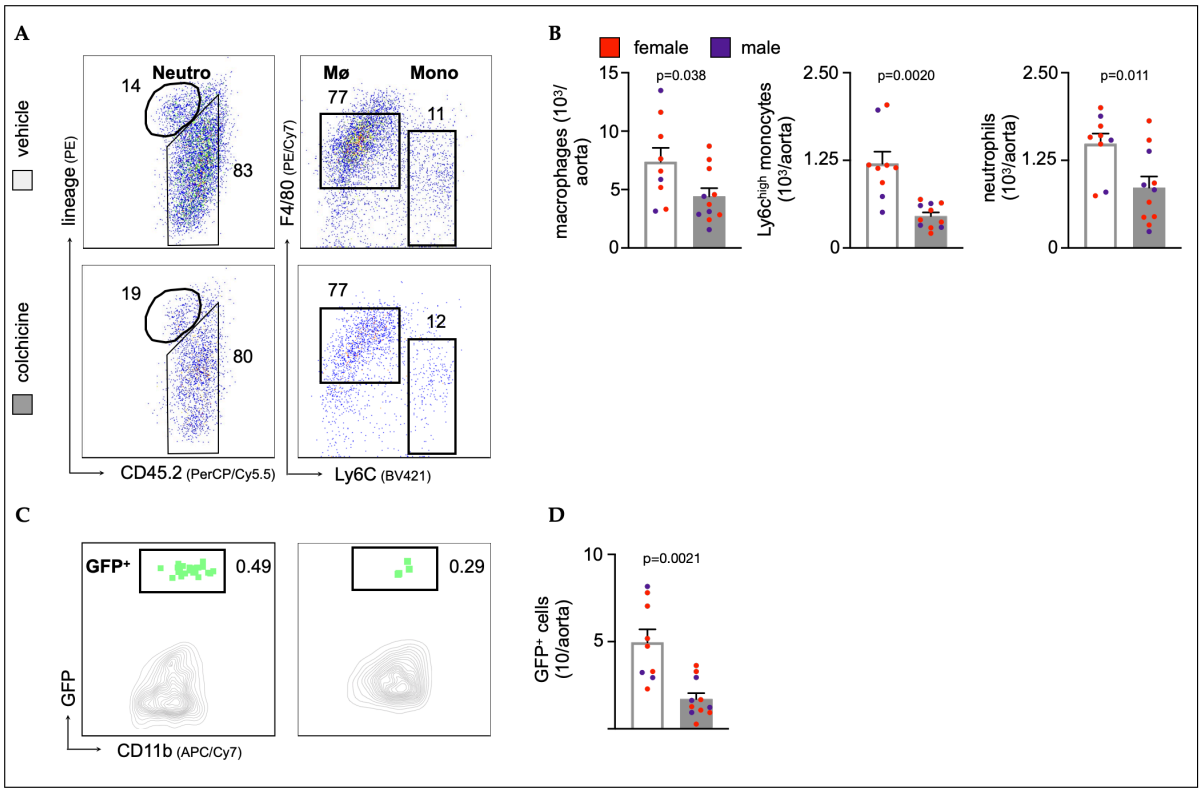

Figure 25: Colchicine treatment reduces vascular inflammation in post-myocardial infarction accelerated atherosclerosis

(A) Flow cytometric gating and **(B)** quantification of leukocyte subsets in atherosclerotic aortas in vehicle- vs. colchicine-treated *Apoe*$^{-/-}$ mice which underwent myocardial infarction 5 weeks prior (n=9-11 per group, 64-67% female, Student's t-test for macrophages and neutrophils, Welch's t-test for monocytes). Abbreviations: Neutro: neutrophils, Mø: macrophages and Mono: monocytes. **(C)** Flow cytometric gating and **(D)** quantification of GFP^{high} myeloid cells (GFP^{+}) in atherosclerotic aortas 24 h after adoptive transfer of GFP^{high} monocytes and neutrophils into vehicle- vs.colchicine-treated *Apoe*$^{-/-}$ mice which were infarcted five weeks prior (n=9-11 per group, 64-67% female, Welch's t-test, 64-67%). Data are presented as mean + s.e.m. Numbers next to gates indicate population frequencies (%). Dots within bar plots show the gender of the mice with a color code: purple (male) and

red (female). Reprinted under the terms of the Creative Commons CC BY license: Figure 6B+C+D from reference (Meyer-Lindemann *et al., 2022)*

4 Discussion

Atherosclerosis is a chronic inflammatory disease of the vessel wall. Increased incidence of cardiovascular risk factors – above all obesity and type 2 diabetes – have drastically enhanced the occurrence of cardiovascular disease both in high-income countries and in the developing world in recent years (Roth *et al.*, 2020). In addition to lifestyle changes, the pharmacological treatment of the disease is primarily operated by interventions addressing high cholesterol levels and arterial hypertension (Visseren *et al.*, 2022). Inflammation, however, was just recently identified as a new target – with the aim of directly attacking disease driving participants of the inflammatory cascade to decelerate progression of disease and eventually improve the patient outcome (Soehnlein and Libby, 2021). To achieve this ambitious goal, colchicine, a well-known drug with anti-inflammatory properties, represents a potential therapeutic option. Best studied in the context of gout, it exerts its anti-inflammatory properties via inhibiting microtubules and thereby suppresses intracellular transport (Deftereos *et al.*, 2013). This – among other factors – leads to reduced formation of one of the key players in promoting inflammation: the NLRP3 inflammasome. Microtubules are essential for the spatial arrangement of its components required for activation (Misawa *et al.*, 2013). The beneficial mode of action of colchicine in the context of CAD was recently demonstrated in LoDoCo2 and COLCOT, where the drug managed to reduce cardiovascular events among patients with recent acute coronary syndrome and chronic coronary disease (Tardif *et al.*, 2019, Nidorf *et al.*, 2020a). However, it remains unclear how anti-inflammatory colchicine modulates the course of CVD in a favorable way. In this thesis, it was demonstrated that colchicine prevents progression of atherosclerosis through a reduction of plaque inflammation by narrowing the recruitment capacities of blood neutrophils and monocytes.

4.1 Colchicine reduced plaque inflammation

Driving forces of plaque inflammation include the accumulation of inflammatory cells and the secretion of proinflammatory, disease-propagating cytokines.

4.1.1 …by decreasing accumulation of inflammatory cells

Flow cytometry as well as immunohistochemistry analyses revealed a colchicine-induced reduction of inflammatory leukocytes within aortic plaques in both early and MI-accelerated atherosclerosis. A depletion of leukocytes is equivalent to a reduced inflammatory environment which ultimately decelerates atherosclerosis progression (Swirski and Nahrendorf, 2013, Soehnlein and Libby, 2021). Complementary to our data, it was previously shown that colchicine does not only reduce inflammatory cells to tame inflammation, but also shifts the phenotype of macrophages from the pro-inflammatory (M1) to the anti-inflammatory (M2) type (Sukeishi *et al.*, 2017, Wang *et al.*, 2021).

4.1.2 …by dampening expression of inflammatory cytokines inside plaques

By evaluating gene expression in aortic arches of colchicine-treated mice, diminished levels of *TNF-alpha* transcripts were detected. TNF-alpha is one of the most potent pro-inflammatory cytokines and plays a pivotal role in the inflammatory cascade. In advanced atherosclerosis, TNF-alpha shifts lesions to a more advanced phenotype by promoting necrosis and reducing apoptosis (Boesten *et al.*, 2005). Consistent with the results of this thesis, it was previously shown that colchicine can inhibit LPS-induced TNF-alpha production in both rat peritoneal macrophages and human blood monocytes (Allen *et al.*, 1991, Li *et al.*, 1996). Regarding the genetic expression of interleukins in aortas, no colchicine-related changes were detected. In concert with results described in this thesis, recently published data also revealed no differences concerning pro-inflammatory cytokine levels either (Roubille *et al.*, 2021). However, colchicine completely blocked maturation of Il-1ß after activating the NLRP3 inflammasome in a monocyte cell line using urate crystals (Martinon *et al.*, 2006). In fact, it is well known that colchicine has the capability to inhibit the NLRP3 inflammasome resulting in diminished cytokine release (Park *et al.*, 2016). Just recently, the analysis of serum from 278 patients participating in LoDoCo2 elicited lower levels of the NLRP3 inflammasome in extracellular vesicles in colchicine-treated patients (Silvis *et al.*, 2021). As only whole aortic arches were analyzed in this thesis, it is not possible to distinguish whether colchicine affects the genetic expression of interleukins in different cell types/ subsets. Further, it was not investigated whether colchicine influences the genetic expression of the NLRP3 inflammasome in

macrophages. Thus, more research is required to further characterize the effect of colchicine on pro-inflammatory cytokines in the context of atherosclerosis. Nevertheless, this work clearly illustrates that colchicine reduces accumulation of inflammatory leukocytes. Combined with the abatement of TNF-alpha in aortic arches, these data indicate that colchicine succeeds in reducing plaque inflammation.

4.2 Colchicine treatment promoted plaque stability

By characterizing the architecture of aortic atherosclerotic plaques, two prognostic factors mainly influencing the outcome of atherosclerosis were analyzed: i) plaque size, i.e., the extent of lumen narrowing and ii) plaque composition, indicating the risk for plaque erosion/ rupture. Plaque stability is mainly promoted by the fibrous cap, the protective coat of the plaque. The fibrous cap is formed by proliferating smooth muscle cells and ECM (Hu *et al.*, 2019, Libby *et al.*, 2019a). MMPS compromise plaque stability by proteolytic degradation of the extracellular matrix (ECM) (Brew and Nagase, 2010). The histological evaluation of the aortic arch showed reduced lesion burden with smaller plaques in colchicine-treated mice. Besides, the quantification of gene expression in the aortic arch showed fewer transcripts of *MMP3*, *MMP9*, and *MMP10* in colchicine-treated mice, thereby indicating improved plaque stability (Frodermann and Nahrendorf, 2018). Clearly, lower-grade stenoses that are less prone to rupture reduce the incidence of complications associated with atherosclerosis. In line with the data presented in this thesis, it was recently described that colchicine decreases plaque vulnerability with reductions in plaque inflammation, medial fibrosis, and outwards vascular remodeling in a rabbit model (Roubille *et al.*, 2021).

4.3 Colchicine treatment attenuated plaque leukocyte recruitment

Knowing that anti-inflammatory colchicine diminishes the expansion of leukocytes in atherosclerotic plaques, the next step was to explore which part of the leukocyte supply chain is affected. As the underlying cause, a diminished recruitment of neutrophils and

monocytes into aortic plaques was identified. Recruitment is a complex interplay, predominantly executed by ECs and circulating leukocytes. Leukocyte trafficking experiments revealed a lower uptake of adoptively transferred GPF^{high} leukocytes into atherosclerotic mice. To further describe and better comprehend this effect, cells were purified by fluorescent-cell activated sorting and mRNA levels of their adhesion molecules, chemokines, and integrins were compared. Here, no effect of colchicine on ECs was observed. Contrarily, previously published studies showed that colchicine decreases or alters the expression of endothelial adhesion molecules. Application of colchicine (10, 50 µM) on human umbilical vein ECs (HUVECS) led to a significant downregulation of ICAM-1 and E-Selectin expression (Perico *et al.*, 1996). Further, an altered distribution of E-Selectin on ECs was observed after application of colchicine (3 nM) *in vitro* (Cronstein *et al.*, 1995). However, the comparability of these studies with the data presented in this thesis is difficult, as different dosages of colchicine were applied in divergent settings (*in vivo vs. in vitro*).

4.3.1 …by silencing neutrophil and monocyte activation

To better understand how colchicine diminishes leukocyte recruitment, the second protagonist of recruitment was investigated: leukocytes. Here, these data demonstrate that colchicine leads to substantial changes in mRNA levels of adhesion molecules, chemokines and integrins of both neutrophils and Ly6C^{high} monocytes. Surface markers like L-Selectin – crucial for neutrophil chemotaxis and monocytic recruitment – were significantly downregulated on both monocytes and neutrophils. Concordantly, a colchicine-reduced expression of L-Selectin on neutrophils and lymphocytes was previously described (Cronstein *et al.*, 1995, Perico *et al.*, 1996). Neutrophils have long played a minor role in atherosclerosis research, even though the number of circulating neutrophils is long known to correlate with the occurrence of cardiovascular events (Friedman *et al.*, 1974). Indeed, neutrophils are not only essential for the recruitment of monocytes, but are also vitally important for the activation of macrophages (Silvestre-Roig *et al.*, 2020). Secretion of neutrophil extracellular traps (NET) activates the NLRP3 inflammasome in macrophages and consequently triggers the production of IL-1ß (Soehnlein and Libby, 2021). Recently, it was shown that colchicine reduces NET formation, eventually leading to lower cytokine

release from neutrophils (Vaidya *et al.*, 2021). In contrast to neutrophils, monocytes are the classical leukocyte subset associated with atherosclerosis. Once migrated into plaques, they locally differentiate into macrophages and fulfill their role as disease-driving cells by exercising numerous proatherogenic functions including lipid retention (Libby *et al.*, 2019a). For the initial recruitment of monocytes, the integrin VLA4 and the chemokines CCR2 and CCR5 are particularly important (Soehnlein *et al.*, 2013). In this thesis, reduced levels of both components of VLA4, ITGA4, and ITGB1, as well as a reduced expression of CCR5 were found, resulting in lower uptake of monocytes. This may also contribute to the observed reduction in plaque size, as experiments specifically targeting CCL2, CXCR1, and CCR2 revealed a 90% reduction in lesion burden (Combadiere *et al.*, 2008). As the data suggested that colchicine predominantly decreases recruitment by altering leukocytes, an *in vivo* "proof of concept" experiment was designed. Here, leukocytes were isolated from GFP-expressing mice previously treated with vehicle or colchicine and were then adoptively transferred into *Apoe*$^{-/-}$ mice. Twenty-four hours later, lower numbers of GFP^{high} leukocytes within aortas were detected. Therefore, the results presented in this thesis strongly suggest that colchicine impairs the recruitment capacities of neutrophils and monocytes into atherosclerotic plaques.

4.4 Colchicine treatment did not affect monocyte-to-macrophage transition or macrophage proliferation

As previously described, monocytes migrate into plaques, locally differentiate into macrophages, which can proliferate *in-situ*. Indispensable for these operations is colony stimulating factor 1 (CSF1), also known as M-CSF (Lin *et al.*, 2019). A reduction of aortic *CSF1* mRNA was observed suggesting an effect of colchicine on monocyte differentiation and/ or proliferation. Knowing that neutralizing CSF1 protects against several inflammatory diseases (Lin *et al.*, 2019), it was attempted to link the hypothesis to a functional level. Thus, the effect of colchicine (0, 1, 10 ng/ml) on BMDM differentiation and proliferation was studied. However, no changes in macrophage numbers were detected *in vitro*. Colchicine, often referred to as mitotic spindle poison, did not impact

macrophage proliferation in this setting. Previously, a reduced proliferation rate of osteoblasts was noted when applying colchicine at concentrations between 10-30 ng/ml (Salai *et al.*, 2001). Taking into consideration that the mode of action of colchicine is dependent on its dosage – colchicine inhibits microtubule formation at low doses, but ensures depolymerization at high doses (Deftereos *et al.*, 2013) – it is most likely, that the clinically relevant dosage chosen in this study was too low to affect macrophage proliferation. Nevertheless, the observed local decrease of *CSF1* in aortas is promising and underlines the atheroprotective properties of colchicine, as CSF1 generated in the vessel wall promotes initiation and progression of atherosclerosis (Rajavashisth *et al.*, 1998).

4.5 Conclusion

Taken together, the results provide comprehensive insights into the influence of colchicine on the inflammatory architecture of atherosclerotic plaques. The data indicate that colchicine prevents expansion of plaque inflammatory leukocytes through lowering recruitment of blood myeloid cells to aortic atherosclerotic plaques. Translationally, the data generated in this thesis contributes to a better understanding of how colchicine reduces the incidence of cardiovascular events in high-risk patients.

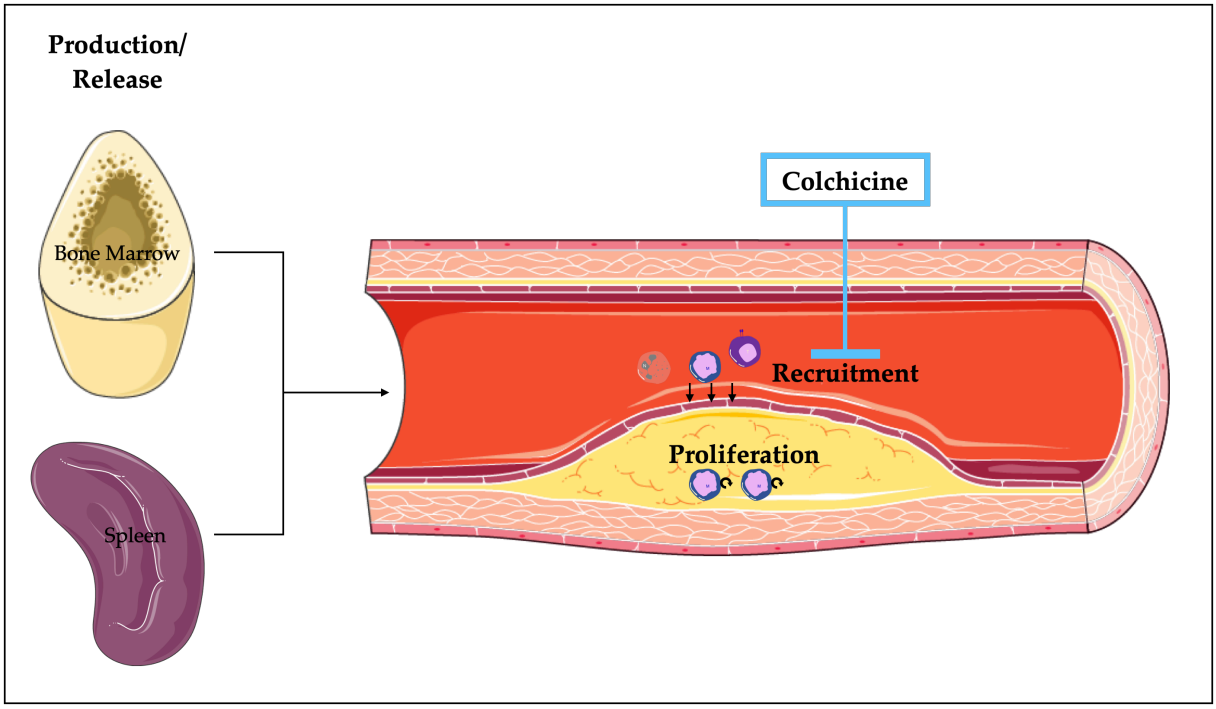

Figure 26: Colchicine beneficially alters atherosclerosis by reducing the recruitment capacities of blood neutrophils and monocytes

5 Bibliography

Abbate, A., Toldo, S., Marchetti, C., Kron, J., Van Tassell, B. W.,Dinarello, C. A. Interleukin-1 and the Inflammasome as Therapeutic Targets in Cardiovascular Disease.Circ Res 2020. 126(9):1260-1280.

Akodad, M., Fauconnier, J., Sicard, P., Huet, F., Blandel, F., Bourret, A., de Santa Barbara, P., Aguilhon, S., LeGall, M., Hugon, G., Lacampagne, A.,Roubille, F. Interest of colchicine in the treatment of acute myocardial infarct responsible for heart failure in a mouse model.Int J Cardiol 2017. 240:347-353.

Allen, J. N., Herzyk, D. J.,Wewers, M. D. Colchicine has opposite effects on interleukin-1 beta and tumor necrosis factor-alpha production.Am J Physiol 1991. 261(4 Pt 1):L315-321.

Bell, J. FDA unconvinced by Novartis pitch for canakinumab.BioPharma Dive 2018.

Boesten, L. S., Zadelaar, A. S., van Nieuwkoop, A., Gijbels, M. J., de Winther, M. P., Havekes, L. M.,van Vlijmen, B. J. Tumor necrosis factor-alpha promotes atherosclerotic lesion progression in APOE*3-Leiden transgenic mice.Cardiovasc Res 2005. 66(1):179-185.

Brew, K.,Nagase, H. The tissue inhibitors of metalloproteinases (TIMPs): an ancient family with structural and functional diversity.Biochim Biophys Acta 2010. 1803(1):55-71.

Burgess, E., Hassmen, P.,Pumpa, K. L. Determinants of adherence to lifestyle intervention in adults with obesity: a systematic review.Clin Obes 2017. 7(3):123-135.

Combadiere, C., Potteaux, S., Rodero, M., Simon, T., Pezard, A., Esposito, B., Merval, R., Proudfoot, A., Tedgui, A.,Mallat, Z. Combined inhibition of CCL2, CX3CR1, and CCR5 abrogates Ly6C(hi) and Ly6C(lo) monocytosis and almost abolishes atherosclerosis in hypercholesterolemic mice.Circulation 2008. 117(13):1649-1657.

Cronstein, B. N., Molad, Y., Reibman, J., Balakhane, E., Levin, R. I.,Weissmann, G. Colchicine alters the quantitative and qualitative display of selectins on endothelial cells and neutrophils.J Clin Invest 1995. 96(2):994-1002.

Deftereos, S., Giannopoulos, G., Papoutsidakis, N., Panagopoulou, V., Kossyvakis, C., Raisakis, K., Cleman, M. W.,Stefanadis, C. Colchicine and the heart: pushing the envelope.J Am Coll Cardiol 2013. 62(20):1817-1825.

Dutta, P., Hoyer, F. F., Grigoryeva, L. S., Sager, H. B., Leuschner, F., Courties, G., Borodovsky, A., Novobrantseva, T., Ruda, V. M., Fitzgerald, K., Iwamoto, Y., Wojtkiewicz, G., Sun, Y., Da Silva, N., Libby, P., Anderson, D. G., Swirski, F. K., Weissleder, R.,Nahrendorf, M. Macrophages retain hematopoietic stem cells in the spleen via VCAM-1.J Exp Med 2015. 212(4):497-512.

Falk, E. Pathogenesis of atherosclerosis.J Am Coll Cardiol 2006. 47(8 Suppl):C7-12.

Fiolet, A. T. L., Opstal, T. S. J., Mosterd, A., Eikelboom, J. W., Jolly, S. S., Keech, A. C., Kelly, P., Tong, D. C., Layland, J., Nidorf, S. M., Thompson, P. L., Budgeon, C., Tijssen, J. G. P.,Cornel, J.

H. Efficacy and safety of low-dose colchicine in patients with coronary disease: a systematic review and meta-analysis of randomized trials.Eur Heart J 2021. 42(28):2765-2775.

Friedman, G. D., Klatsky, A. L.,Siegelaub, A. B. The leukocyte count as a predictor of myocardial infarction.N Engl J Med 1974. 290(23):1275-1278.

Frodermann, V.,Nahrendorf, M. Macrophages and Cardiovascular Health.Physiol Rev 2018. 98(4):2523-2569.

Fujisue, K., Sugamura, K., Kurokawa, H., Matsubara, J., Ishii, M., Izumiya, Y., Kaikita, K.,Sugiyama, S. Colchicine Improves Survival, Left Ventricular Remodeling, and Chronic Cardiac Function After Acute Myocardial Infarction.Circ J 2017. 81(8):1174-1182.

Galley, H. F.,Webster, N. R. Physiology of the endothelium.Br J Anaesth 2004. 93(1):105-113.

Goodson, H. V.,Jonasson, E. M. Microtubules and Microtubule-Associated Proteins.Cold Spring Harb Perspect Biol 2018. 10(6).

Guo, S., Yang, C., Diao, B., Huang, X., Jin, M., Chen, L., Yan, W., Ning, Q., Zheng, L., Wu, Y.,Chen, Y. The NLRP3 Inflammasome and IL-1beta Accelerate Immunologically Mediated Pathology in Experimental Viral Fulminant Hepatitis.PLoS Pathog 2015. 11(9):e1005155.

Hu, D., Yin, C., Luo, S., Habenicht, A. J. R.,Mohanta, S. K. Vascular Smooth Muscle Cells Contribute to Atherosclerosis Immunity.Front Immunol 2019. 10:1101.

Karasawa, T.,Takahashi, M. Role of NLRP3 Inflammasomes in Atherosclerosis.J Atheroscler Thromb 2017. 24(5):443-451.

Kleemann, R., Zadelaar, S.,Kooistra, T. Cytokines and atherosclerosis: a comprehensive review of studies in mice.Cardiovasc Res 2008. 79(3):360-376.

Ley, K.,Reutershan, J. Leucocyte-endothelial interactions in health and disease.Handb Exp Pharmacol 2006. (176 Pt 2):97-133.

Li, Z., Davis, G. S., Mohr, C., Nain, M.,Gemsa, D. Inhibition of LPS-induced tumor necrosis factor-alpha production by colchicine and other microtubule disrupting drugs.Immunobiology 1996. 195(4-5):624-639.

Li, Z. Y., Howarth, S. P., Tang, T.,Gillard, J. H. How critical is fibrous cap thickness to carotid plaque stability? A flow-plaque interaction model.Stroke 2006. 37(5):1195-1199.

Libby, P., Buring, J. E., Badimon, L., Hansson, G. K., Deanfield, J., Bittencourt, M. S., Tokgozoglu, L.,Lewis, E. F. Atherosclerosis.Nat Rev Dis Primers 2019a. 5(1):56.

Libby, P.,Everett, B. M. Novel Antiatherosclerotic Therapies.Arterioscler Thromb Vasc Biol 2019. 39(4):538-545.

Libby, P., Pasterkamp, G., Crea, F.,Jang, I. K. Reassessing the Mechanisms of Acute Coronary Syndromes.Circ Res 2019b. 124(1):150-160.

Libby, P., Ridker, P. M., Hansson, G. K.,Leducq Transatlantic Network on, A. Inflammation in atherosclerosis: from pathophysiology to practice.J Am Coll Cardiol 2009. 54(23):2129-2138.

Lin, W., Xu, D., Austin, C. D., Caplazi, P., Senger, K., Sun, Y., Jeet, S., Young, J., Delarosa, D., Suto, E., Huang, Z., Zhang, J., Yan, D., Corzo, C., Barck, K., Rajan, S., Looney, C., Gandham, V., Lesch, J., Liang, W. C., Mai, E., Ngu, H., Ratti, N., Chen, Y., Misner, D., Lin, T., Danilenko, D., Katavolos, P., Doudemont, E., Uppal, H., Eastham, J., Mak, J., de Almeida, P. E., Bao, K., Hadadianpour, A., Keir, M., Carano, R. A. D., Diehl, L., Xu, M., Wu, Y., Weimer, R. M., DeVoss, J., Lee, W. P., Balazs, M., Walsh, K., Alatsis, K. R., Martin, F.,Zarrin, A. A. Function of CSF1 and IL34 in Macrophage Homeostasis, Inflammation, and Cancer.Front Immunol 2019. 10:2019.

Lo Sasso, G., Schlage, W. K., Boue, S., Veljkovic, E., Peitsch, M. C.,Hoeng, J. The Apoe(-/-) mouse model: a suitable model to study cardiovascular and respiratory diseases in the context of cigarette smoke exposure and harm reduction.J Transl Med 2016. 14(1):146.

Madjid, M., Awan, I., Willerson, J. T.,Casscells, S. W. Leukocyte count and coronary heart disease: implications for risk assessment.J Am Coll Cardiol 2004. 44(10):1945-1956.

Martinon, F., Petrilli, V., Mayor, A., Tardivel, A.,Tschopp, J. Gout-associated uric acid crystals activate the NALP3 inflammasome.Nature 2006. 440(7081):237-241.

Mauersberger, C., Hinterdobler, J., Schunkert, H., Kessler, T.,Sager, H. B. Where the Action Is-Leukocyte Recruitment in Atherosclerosis.Front Cardiovasc Med 2021. 8:813984.

Meyer-Lindemann, U., Mauersberger, C., Schmidt, A. C., Moggio, A., Hinterdobler, J., Li, X., Khangholi, D., Hettwer, J., Grasser, C., Dutsch, A., Schunkert, H., Kessler, T.,Sager, H. B. Colchicine Impacts Leukocyte Trafficking in Atherosclerosis and Reduces Vascular Inflammation.Front Immunol 2022. 13:898690.

Misawa, T., Takahama, M., Kozaki, T., Lee, H., Zou, J., Saitoh, T.,Akira, S. Microtubule-driven spatial arrangement of mitochondria promotes activation of the NLRP3 inflammasome.Nat Immunol 2013. 14(5):454-460.

Nahrendorf, M.,Swirski, F. K. Lifestyle effects on hematopoiesis and atherosclerosis.Circ Res 2015. 116(5):884-894.

Nidorf, S. M., Fiolet, A. T. L., Mosterd, A., Eikelboom, J. W., Schut, A., Opstal, T. S. J., The, S. H. K., Xu, X. F., Ireland, M. A., Lenderink, T., Latchem, D., Hoogslag, P., Jerzewski, A., Nierop, P., Whelan, A., Hendriks, R., Swart, H., Schaap, J., Kuijper, A. F. M., van Hessen, M. W. J., Saklani, P., Tan, I., Thompson, A. G., Morton, A., Judkins, C., Bax, W. A., Dirksen, M., Alings, M., Hankey, G. J., Budgeon, C. A., Tijssen, J. G. P., Cornel, J. H., Thompson, P. L.,LoDoCo2 Trial, I. Colchicine in Patients with Chronic Coronary Disease.N Engl J Med 2020a. 383(19):1838-1847.

Nidorf, S. M., Fiolet, A. T. L., Mosterd, A., Eikelboom, J. W., Schut, A., Opstal, T. S. J., The, S. H. K., Xu, X. F., Ireland, M. A., Lenderink, T., Latchem, D., Hoogslag, P., Jerzewski, A., Nierop, P., Whelan, A., Hendriks, R., Swart, H., Schaap, J., Kuijper, A. F. M., van Hessen, M. W. J., Saklani, P., Tan, I., Thompson, A. G., Morton, A., Judkins, C., Bax, W. A., Dirksen, M., Alings, M. M. W., Hankey, G. J., Budgeon, C. A., Tijssen, J. G. P., Cornel, J. H., Thompson, P.

L.,LoDoCo2 Trial, I. Colchicine in Patients with Chronic Coronary Disease.N Engl J Med 2020b.

Nidorf, S. M.,Thompson, P. L. Why Colchicine Should Be Considered for Secondary Prevention of Atherosclerosis: An Overview.Clin Ther 2019. 41(1):41-48.

Park, Y. H., Wood, G., Kastner, D. L.,Chae, J. J. Pyrin inflammasome activation and RhoA signaling in the autoinflammatory diseases FMF and HIDS.Nat Immunol 2016. 17(8):914-921.

Pascart, T.,Richette, P. Colchicine in Gout: An Update.Curr Pharm Des 2018. 24(6):684-689.

Perico, N., Ostermann, D., Bontempeill, M., Morigi, M., Amuchastegui, C. S., Zoja, C., Akalin, E., Sayegh, M. H.,Remuzzi, G. Colchicine interferes with L-selectin and leukocyte function-associated antigen-1 expression on human T lymphocytes and inhibits T cell activation.J Am Soc Nephrol 1996. 7(4):594-601.

Rajavashisth, T., Qiao, J. H., Tripathi, S., Tripathi, J., Mishra, N., Hua, M., Wang, X. P., Loussararian, A., Clinton, S., Libby, P.,Lusis, A. Heterozygous osteopetrotic (op) mutation reduces atherosclerosis in LDL receptor- deficient mice.J Clin Invest 1998. 101(12):2702-2710.

Ramji, D. P.,Davies, T. S. Cytokines in atherosclerosis: Key players in all stages of disease and promising therapeutic targets.Cytokine Growth Factor Rev 2015. 26(6):673-685.

Rathinam, V. A.,Fitzgerald, K. A. Inflammasome Complexes: Emerging Mechanisms and Effector Functions.Cell 2016. 165(4):792-800.

Ridker, P. M., Everett, B. M., Thuren, T., MacFadyen, J. G., Chang, W. H., Ballantyne, C., Fonseca, F., Nicolau, J., Koenig, W., Anker, S. D., Kastelein, J. J. P., Cornel, J. H., Pais, P., Pella, D., Genest, J., Cifkova, R., Lorenzatti, A., Forster, T., Kobalava, Z., Vida-Simiti, L., Flather, M., Shimokawa, H., Ogawa, H., Dellborg, M., Rossi, P. R. F., Troquay, R. P. T., Libby, P., Glynn, R. J.,Group, C. T. Antiinflammatory Therapy with Canakinumab for Atherosclerotic Disease.N Engl J Med 2017. 377(12):1119-1131.

Ridker, P. M., MacFadyen, J. G., Everett, B. M., Libby, P., Thuren, T., Glynn, R. J.,Group, C. T. Relationship of C-reactive protein reduction to cardiovascular event reduction following treatment with canakinumab: a secondary analysis from the CANTOS randomised controlled trial.Lancet 2018. 391(10118):319-328.

Robbins, C. S., Chudnovskiy, A., Rauch, P. J., Figueiredo, J. L., Iwamoto, Y., Gorbatov, R., Etzrodt, M., Weber, G. F., Ueno, T., van Rooijen, N., Mulligan-Kehoe, M. J., Libby, P., Nahrendorf, M., Pittet, M. J., Weissleder, R.,Swirski, F. K. Extramedullary hematopoiesis generates Ly-6C(high) monocytes that infiltrate atherosclerotic lesions.Circulation 2012. 125(2):364-374.

Roth, G. A., Mensah, G. A., Johnson, C. O., Addolorato, G., Ammirati, E., Baddour, L. M., Barengo, N. C., Beaton, A. Z., Benjamin, E. J., Benziger, C. P., Bonny, A., Brauer, M., Brodmann, M., Cahill, T. J., Carapetis, J., Catapano, A. L., Chugh, S. S., Cooper, L. T., Coresh, J., Criqui, M., DeCleene, N., Eagle, K. A., Emmons-Bell, S., Feigin, V. L., Fernandez-Sola, J., Fowkes, G., Gakidou, E., Grundy, S. M., He, F. J., Howard, G., Hu, F., Inker, L., Karthikeyan, G., Kassebaum, N., Koroshetz, W., Lavie, C., Lloyd-Jones, D., Lu, H. S., Mirijello, A., Temesgen,

A. M., Mokdad, A., Moran, A. E., Muntner, P., Narula, J., Neal, B., Ntsekhe, M., Moraes de Oliveira, G., Otto, C., Owolabi, M., Pratt, M., Rajagopalan, S., Reitsma, M., Ribeiro, A. L. P., Rigotti, N., Rodgers, A., Sable, C., Shakil, S., Sliwa-Hahnle, K., Stark, B., Sundstrom, J., Timpel, P., Tleyjeh, I. M., Valgimigli, M., Vos, T., Whelton, P. K., Yacoub, M., Zuhlke, L., Murray, C., Fuster, V.,Group, G.-N.-J. G. B. o. C. D. W. Global Burden of Cardiovascular Diseases and Risk Factors, 1990-2019: Update From the GBD 2019 Study.J Am Coll Cardiol 2020. 76(25):2982-3021.

Roubille, F., Merlet, N., Busseuil, D., Ferron, M., Shi, Y., Mihalache-Avram, T., Mecteau, M., Brand, G., Rivas, D., Cossette, M., Guertin, M.-C., Rhéaume, E.,Tardif, J.-C. Colchicine reduces atherosclerotic plaque vulnerability in rabbits.Atherosclerosis Plus 2021. 45:1-9.

Salai, M., Segal, E., Cohen, I., Dudkiewicz, I., Farzame, N., Pitaru, S.,Savion, N. The inhibitory effects of colchicine on cell proliferation and mineralisation in culture.J Bone Joint Surg Br 2001. 83(6):912-915.

Samuel, M., Tardif, J. C., Khairy, P., Roubille, F., Waters, D. D., Gregoire, J. C., Pinto, F. J., Maggioni, A. P., Diaz, R., Berry, C., Koenig, W., Ostadal, P., Lopez-Sendon, J., Gamra, H., Kiwan, G. S., Dube, M. P., Provencher, M., Orfanos, A., Blondeau, L., Kouz, S., L'Allier, P. L., Ibrahim, R., Bouabdallaoui, N., Mitchell, D., Guertin, M. C.,Lelorier, J. Cost-effectiveness of low-dose colchicine after myocardial infarction in the Colchicine Cardiovascular Outcomes Trial (COLCOT).Eur Heart J Qual Care Clin Outcomes 2021. 7(5):486-495.

Silvestre-Roig, C., Braster, Q., Ortega-Gomez, A.,Soehnlein, O. Neutrophils as regulators of cardiovascular inflammation.Nat Rev Cardiol 2020. 17(6):327-340.

Silvis, M. J. M., Fiolet, A. T. L., Opstal, T. S. J., Dekker, M., Suquilanda, D., Zivkovic, M., Duyvendak, M., The, S. H. K., Timmers, L., Bax, W. A., Mosterd, A., Cornel, J. H.,de Kleijn, D. P. V. Colchicine reduces extracellular vesicle NLRP3 inflammasome protein levels in chronic coronary disease: A LoDoCo2 biomarker substudy.Atherosclerosis 2021. 334:93-100.

Soehnlein, O., Drechsler, M., Doring, Y., Lievens, D., Hartwig, H., Kemmerich, K., Ortega-Gomez, A., Mandl, M., Vijayan, S., Projahn, D., Garlichs, C. D., Koenen, R. R., Hristov, M., Lutgens, E., Zernecke, A.,Weber, C. Distinct functions of chemokine receptor axes in the atherogenic mobilization and recruitment of classical monocytes.EMBO Mol Med 2013. 5(3):471-481.

Soehnlein, O.,Libby, P. Targeting inflammation in atherosclerosis - from experimental insights to the clinic.Nat Rev Drug Discov 2021. 20(8):589-610.

Strandberg, T. E.,Kovanen, P. T. Coronary artery disease: 'gout' in the artery?Eur Heart J 2021. 42(28):2761-2764.

Sukeishi, A., Isami, K., Hiyama, H., Imai, S., Nagayasu, K., Shirakawa, H., Nakagawa, T.,Kaneko, S. Colchicine alleviates acute postoperative pain but delays wound repair in mice: roles of neutrophils and macrophages.Mol Pain 2017. 13:1744806917743680.

Swirski, F. K.,Nahrendorf, M. Leukocyte behavior in atherosclerosis, myocardial infarction, and heart failure.Science 2013. 339(6116):161-166.

Tardif, J.-C., Kouz, S., Waters, D. D., Bertrand, O. F., Diaz, R., Maggioni, A. P., Pinto, F. J., Ibrahim, R., Gamra, H., Kiwan, G. S., Berry, C., López-Sendón, J., Ostadal, P., Koenig, W., Angoulvant, D., Grégoire, J. C., Lavoie, M.-A., Dubé, M.-P., Rhainds, D., Provencher, M., Blondeau, L., Orfanos, A., L'Allier, P. L., Guertin, M.-C.,Roubille, F. Efficacy and Safety of Low-Dose Colchicine after Myocardial Infarction.N Engl J Med 2019. 381(26):2497-2505.

Vaidya, K., Tucker, B., Kurup, R., Khandkar, C., Pandzic, E., Barraclough, J., Machet, J., Misra, A., Kavurma, M., Martinez, G., Rye, K. A., Cochran, B. J.,Patel, S. Colchicine Inhibits Neutrophil Extracellular Trap Formation in Patients With Acute Coronary Syndrome After Percutaneous Coronary Intervention.J Am Heart Assoc 2021. 10(1):e018993.

Visseren, F. L. J., Mach, F., Smulders, Y. M., Carballo, D., Koskinas, K. C., Back, M., Benetos, A., Biffi, A., Boavida, J. M., Capodanno, D., Cosyns, B., Crawford, C., Davos, C. H., Desormais, I., Angelantonio, E. D., Franco, O. H., Halvorsen, S., Richard Hobbs, F. D., Hollander, M., Jankowska, E. A., Michal, M., Sacco, S., Sattar, N., Tokgozoglu, L., Tonstad, S., Tsioufis, K. P., van Dis, I., van Gelder, I. C., Wanner, C., Williams, B.,Group, E. S. C. S. D. 2021 ESC Guidelines on cardiovascular disease prevention in clinical practice: Developed by the Task Force for cardiovascular disease prevention in clinical practice with representatives of the European Society of Cardiology and 12 medical societies With the special contribution of the European Association of Preventive Cardiology (EAPC).Rev Esp Cardiol (Engl Ed) 2022. 75(5):429.

Wang, L., Peng, Y., Song, L., Xia, D., Li, C., Li, Z., Li, Q., Yu, A., Lu, C.,Wang, Y. Colchicine-Containing Nanoparticles Attenuates Acute Myocardial Infarction Injury by Inhibiting Inflammation.Cardiovasc Drugs Ther 2021.

Wolf, D.,Ley, K. Immunity and Inflammation in Atherosclerosis.Circ Res 2019. 124(2):315-327.

Yu, X. H., Fu, Y. C., Zhang, D. W., Yin, K.,Tang, C. K. Foam cells in atherosclerosis.Clin Chim Acta 2013. 424:245-252.

Zernecke, A., Winkels, H., Cochain, C., Williams, J. W., Wolf, D., Soehnlein, O., Robbins, C. S., Monaco, C., Park, I., McNamara, C. A., Binder, C. J., Cybulsky, M. I., Scipione, C. A., Hedrick, C. C., Galkina, E. V., Kyaw, T., Ghosheh, Y., Dinh, H. Q.,Ley, K. Meta-Analysis of Leukocyte Diversity in Atherosclerotic Mouse Aortas.Circ Res 2020. 127(3):402-426.

6 Acknowledgement

I would like to thank my supervisor Prof. Dr. Hendrik Sager for his excellent guidance throughout the thesis. His knowledge, enthusiasm and passion for research really inspired me and I am very happy that we will continue to work together in the future. Furthermore, I would like to thank Prof. Dr. Heribert Schunkert for his always valuable and helpful feedback, that made it possible to make progress.

I am grateful to all those with whom I had the opportunity to work during this project. The team spirit in our group is truly unique. I would like to thank Carina Mauersberger for her constant support, her careful and conscientious supervision at all times and especially for the great working atmosphere. I could not have imagined a better companion and I will truly miss our collaboration. I would like to thank Julia Hinterdobler, Simin Schott and Aldo Moggio for the always appreciative and motivating teamwork, and the many helpful pieces of advice.

Last but not least, I would like to thank all the people who have a special place in my heart – my parents, my brothers, Alex, Paulina, Zora, and all my amazing friends.